



Lawrence Berkeley Laboratory

UNIVERSITY OF CALIFORNIA

Physics Division

Submitted to Physical Review D

Testing Supersymmetry at the Next Linear Collider

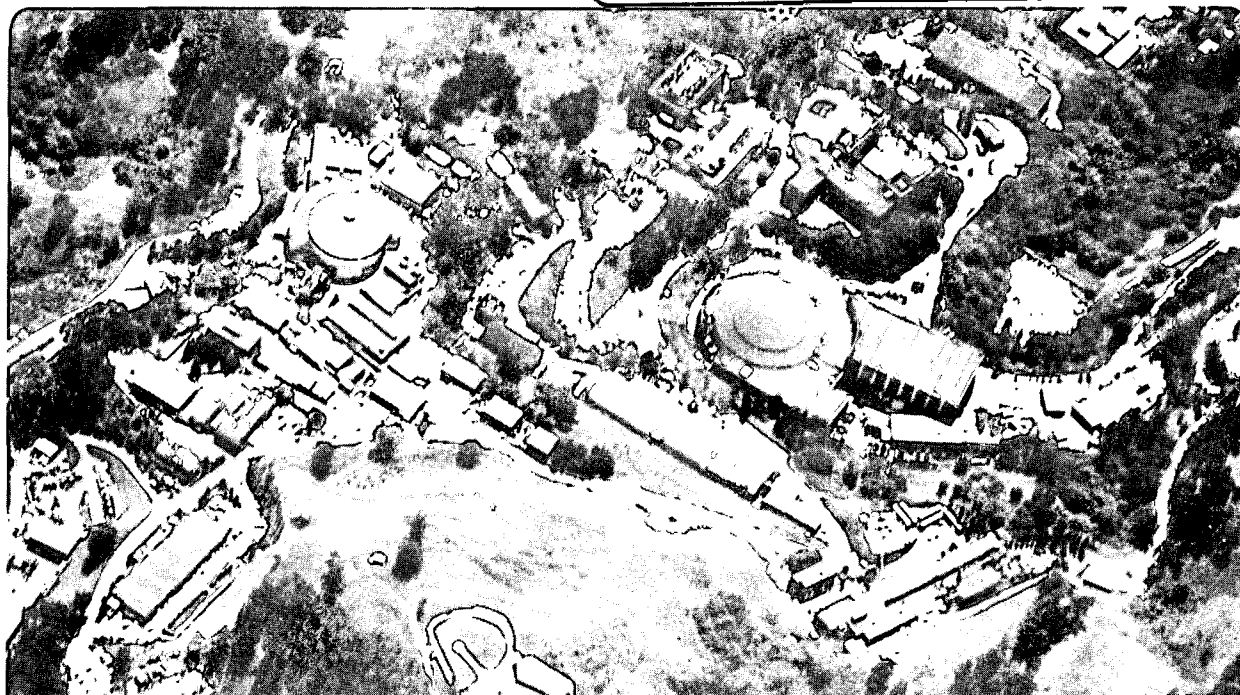
J.L. Feng, M.E. Peskin, H. Murayama, and X. Tata

February 1995

U. C. Lawrence Berkeley Laboratory
Library, Berkeley

FOR REFERENCE

Not to be taken from this room



REFERENCE COPY
Does Not
Circulate

Bldg. 50 Library.

LBL-36101

Copy 1

DISCLAIMER

This document was prepared as an account of work sponsored by the United States Government. While this document is believed to contain correct information, neither the United States Government nor any agency thereof, nor the Regents of the University of California, nor any of their employees, makes any warranty, express or implied, or assumes any legal responsibility for the accuracy, completeness, or usefulness of any information, apparatus, product, or process disclosed, or represents that its use would not infringe privately owned rights. Reference herein to any specific commercial product, process, or service by its trade name, trademark, manufacturer, or otherwise, does not necessarily constitute or imply its endorsement, recommendation, or favoring by the United States Government or any agency thereof, or the Regents of the University of California. The views and opinions of authors expressed herein do not necessarily state or reflect those of the United States Government or any agency thereof or the Regents of the University of California.

Testing Supersymmetry at the Next Linear Collider

J. L. Feng * † and M. E. Peskin *

*Stanford Linear Accelerator Center
Stanford University, Stanford, California 94309*

H. Murayama ‡

*Theoretical Physics Group, Lawrence Berkeley Laboratory
University of California, Berkeley, California 94720*

X. Tata §

*Department of Physics and Astronomy
University of Hawaii, Honolulu, Hawaii 96822*

Up to now, almost all discussion of supersymmetry at future colliders has been concerned with particle searches. However, if candidates for supersymmetric particles are found, there is much more that we will want to know about them. Supersymmetry predicts quantitative relations among the couplings and masses of supersymmetric particles. We discuss the prospects for testing such relations at a future e^+e^- linear collider, using measurements that exploit the availability of polarized beams. Precision tests from chargino production are investigated in two representative cases, and sfermion and neutralino processes are also discussed.

(Submitted to Physical Review D)

*Work supported by the Department of Energy, contract DE-AC03-76SF00515.

†Work supported in part by an NSF Graduate Research Fellowship.

‡Work supported by the Director, Office of Energy Research, Office of High Energy and Nuclear Physics, Division of High Energy Physics of the U.S. Department of Energy under contract DE-AC03-76SF00098.

§Work supported by the Department of Energy, contract DE-FG-03-94ER40833.

I. INTRODUCTION

The phenomenological predictions of supersymmetry (SUSY) may be divided into three categories: (I) reflections of the supersymmetric Lagrangian in standard model phenomenology, including relations among the gauge coupling constants from SUSY grand unification and the presence of a heavy top quark and a light Higgs scalar; (II) the prediction of new particles with the correct spin and quantum number assignments to be superpartners of the standard model particles; and (III) well-defined quantitative relations among the couplings and masses of these new particles. While the predictions of (I) are of great interest, their verification is clearly no substitute for direct evidence. The discovery of a large number of particles in category (II) would be strong support for SUSY. On the other hand, the most compelling confirmation of SUSY would likely be the precise verification of the relations of category (III). This would be especially true if, initially, only a small set of candidate SUSY partners are observed.

Most discussions of supersymmetry at future high-energy colliders have concentrated single-mindedly on the question of particle searches. From one point of view, this is reasonable, because the existence of SUSY partners is unproven and this a prerequisite for any further analysis. On the other hand, the discovery of the first evidence for SUSY — or for any other theoretical extension of the standard model — will begin a program of detailed experimental investigation of the new sector of particles required by this extension. This investigation will need to be carried out with the same experimental tools that were used to make the original discovery. Thus, it is not only reasonable but also crucial, as we plan for the colliders of the next decade, to ask how any new physics that might be discovered can be examined in detail at these machines.

Supersymmetry provides a particularly interesting subject for studies of the detailed analysis of physics beyond the standard model. SUSY models are weakly coupled, so their consequences can be worked out straightforwardly using perturbative computations. At the same time, SUSY models depend on a large number of unknown parameters, and different choices for these parameters yield qualitatively different realizations of possible new physics. Thus, the phenomenology of SUSY is quite complex. Eventually, if SUSY does give a correct model of Nature, the colliders of the next generation will be expected to determine the SUSY parameters, and their values will become clues that take us a step closer to a fundamental theory. We suggest that similar complexity should be found in any realistic extension of the standard model, and that similar investigations will be needed to understand the next, more fundamental, level.

One consequence of the complexity of the parameter space of SUSY models is that it is not trivial to identify experimentally the specific quantities which are related by supersymmetry. Faraggi, Hagelin, Kelley, and Nanopoulos [1], Martin and Ramond [2], and Kawamura, Murayama, and Yamaguchi [3] have discussed in general terms the exploration of the spectroscopy of supersymmetry partners, and the latter two groups have suggested particular mass relations which test supersymmetry independently of more detailed hypotheses. These tests are very ambitious, since they require mass measurements for the heaviest and most elusive particles of the superspectrum — the squarks, the heaviest partners of the Higgs and gauge bosons, and the sneutrino — at the 1% level. In these papers, very little attention was given to the question of how these experiments will be done. In this paper, we will present

some alternative tests of supersymmetry that involve only the lightest observable states of the superspectrum, and we will argue that these should be straightforward to carry out at colliders of the next generation.

Our tests will exploit the advantages of the proposed Next Linear Collider (NLC), a linear e^+e^- collider with $\sqrt{s} = 500 \text{ GeV}$ and a design luminosity of $50 \text{ fb}^{-1}/\text{year}$ [4]. This machine has already been shown to be a powerful tool for probing new physics [5–8]. In particular, previous work has shown that such a machine provides an excellent environment for measuring SUSY parameters under the assumption that newly discovered particles are sparticles [9–15]. In this paper, we add to this body of work by showing how to test this assumption. Our analysis will take into account the relation of observable properties of the final state to the underlying reaction; as in the earlier NLC studies, we will be helped dramatically by the clean experimental environment expected at this machine. In addition, the expected availability of highly polarized electron beams should provide a powerful diagnostic tool.

This study will be conducted in the context of the minimal supersymmetric standard model (MSSM). It is a reasonable expectation that charginos — the mixed superpartners of W bosons and charged Higgs bosons — will be among the lightest supersymmetric states, and that these will be accessible to the NLC. Thus, we concentrate here on tests of supersymmetry that involve the properties of charginos. The crucial problem we will face is that the mass eigenstates of charginos are in general a mixture of weak eigenstates, and their mixing pattern must be resolved before the quantitative implications of supersymmetry become clear. To understand the experimental aspects of chargino reactions needed in this study, we have studied simulations of chargino production and decay using the parton-level Monte Carlo event generator of Feng and Strassler [16].

The outline of this paper is as follows: In Sec. II we review the properties of charginos within the MSSM and state our assumptions. In Sec. III we divide the parameter space into characteristic regions. In Secs. IV and V, we present two different strategies for supersymmetry tests in two of these regions and analyze the experimental prospects for these tests in particular cases. In Sec. VI, we comment on other possible supersymmetry tests involving the properties of matter scalars and neutralinos. We present our conclusions in Sec. VII.

II. THE MSSM AND OUR ASSUMPTIONS

Though our goal in the studies reported here is to test supersymmetry, we cannot begin without narrowing the phenomenological context. SUSY can, in principle, be realized in many ways. Here we assume that the observed particle content and qualitative phenomenology is that of the minimal supersymmetric extension of the standard model (MSSM), with conserved R-parity and therefore a stable lightest supersymmetric particle (LSP). This is the set of assumptions that is associated with the most commonly studied missing energy signatures for the discovery of candidate supersymmetric particles. R-parity conservation and the existence of only two Higgs doublets will be our two primary assumptions, and will be essential for much of the following analysis. We will also incorporate some minor additional restrictions for simplicity. In this section, we detail these assumptions and define

the basic set of parameters. A more detailed presentation of the MSSM can be found in many reviews [17].

The MSSM includes matter superfields and two Higgs doublet superfields \hat{H}_1 and \hat{H}_2 , which give masses to the isospin $-\frac{1}{2}$ and $\frac{1}{2}$ particles, respectively. These two superfields are coupled in the superpotential through the term $-\mu\epsilon_{ij}\hat{H}_1^i\hat{H}_2^j$, and the ratio of the two Higgs scalar vacuum expectation values is defined to be $\tan\beta \equiv \langle H_2^0 \rangle / \langle H_1^0 \rangle$. The MSSM also contains soft SUSY breaking terms [18,19], which are parametrized by masses m_i for the scalar multiplets and masses M_1 , M_2 , and M_3 for the U(1), SU(2), and SU(3) gauginos. In addition, there are cubic couplings (“A terms”) of Higgs scalars and sfermions. With the assumptions that we will make below, our study will be insensitive to the parameters entering through the A terms.

The Higgsinos and electroweak gauginos of the MSSM mix to form two charginos and four neutralinos. In two-component spinor notation, the chargino mass eigenstates are $\tilde{\chi}_i^+ = V_{ij}\psi_j^+$ and $\tilde{\chi}_i^- = U_{ij}\psi_j^-$, where $(\psi^\pm)^T = (-i\tilde{W}^\pm, \tilde{H}^\pm)$ and, by convention, $m_{\tilde{\chi}_1^\pm} < m_{\tilde{\chi}_2^\pm}$. The matrices V and U diagonalize the mass terms

$$(\psi^-)^T M_{\tilde{\chi}^\pm} \psi^+ + h.c. , \quad (1)$$

where

$$M_{\tilde{\chi}^\pm} = \begin{pmatrix} M_2 & \sqrt{2} M_W \sin\beta \\ \sqrt{2} M_W \cos\beta & \mu \end{pmatrix} . \quad (2)$$

Ignoring some subtleties in this diagonalization having to do with negative mass values and the ordering of the eigenstates (see, for example, the first reference in [17]), V and U are orthogonal matrices which can be parametrized by rotation angles ϕ_+ and ϕ_- . For $\phi_\pm = 0$, the chargino $\tilde{\chi}_1^\pm$ is pure gaugino, and for $\phi_\pm = \frac{\pi}{2}$, $\tilde{\chi}_1^\pm$ is pure Higgsino. The neutralino mass eigenstates are $\tilde{\chi}_i^0 = N_{ij}\psi_j^0$, where $(\psi^0)^T = (-i\tilde{B}, -i\tilde{W}^3, \tilde{H}_1^0, \tilde{H}_2^0)$, and N diagonalizes the mass terms

$$\frac{1}{2}(\psi^0)^T M_{\tilde{\chi}^0} \psi^0 + h.c. , \quad (3)$$

where

$$M_{\tilde{\chi}^0} = \begin{pmatrix} M_1 & 0 & -M_Z \cos\beta \sin\theta_W & M_Z \sin\beta \sin\theta_W \\ 0 & M_2 & M_Z \cos\beta \cos\theta_W & -M_Z \sin\beta \cos\theta_W \\ -M_Z \cos\beta \sin\theta_W & M_Z \cos\beta \cos\theta_W & 0 & -\mu \\ M_Z \sin\beta \sin\theta_W & -M_Z \sin\beta \cos\theta_W & -\mu & 0 \end{pmatrix} . \quad (4)$$

To reduce the large number of arbitrary parameters, we follow Ref. [16] in introducing some additional assumptions. These assumptions are primarily phenomenologically motivated, and, where possible, we avoid assumptions based solely on grand unified theories (GUTs) and supergravity theories. As noted above, we assume R-parity conservation and the presence of a stable LSP, which we identify as the lightest neutralino $\tilde{\chi}_1^0$. In addition, we will ignore the intergenerational mixing in the quark and sfermion sectors, and we will assume that CP -violating phases in the SUSY parameters are negligible. We will also assume that one-loop effects do not introduce large and qualitatively new dependences on

SUSY parameters. If these effects are large but may be absorbed by redefinitions of the tree level parameters, our analysis can be applied with only minor modifications. The assumptions listed above will be in effect throughout this study. Additional conditions that are appropriate to the study of specific processes and scenarios will be given below.

III. THE PARAMETER SPACE OF CHARGINOS

In many supersymmetric models, charginos are the lightest observable sparticles, and we now consider the possibilities for tests of SUSY from chargino production. As we are interested in what may be learned from the chargino signal, we will make, in this and the following two sections, the additional assumptions that gluinos, sfermions, and the Higgs scalars H^0 , A^0 , and H^\pm are beyond the kinematic reach of the NLC. Neutralino masses must be comparable to chargino masses, and below we will address the problem of removing neutralino backgrounds to the chargino signal. If a number of additional SUSY signals are available at NLC energies, their detection would be exciting in their own right, and would make possible the measurement of several sparticle masses. However, the procedure we outline below for measuring chargino couplings would not directly apply. Since we think it would be somewhat optimistic to expect a plethora of sparticles to be accessible at NLC energies, we have not explored this scenario further.

The analysis of chargino pair production and decay is discussed in detail in Ref. [16]; here we will only summarize the most important qualitative features of this process. Using the picture of chargino production derived from this analysis, we will divide the parameter space into characteristic regions. In the following two sections, we will define and analyze tests of supersymmetry which rely on the particular characteristics of the chargino in each of these regions.

Though the observables we will discuss involve only the chargino pair production cross section, the problems of experimental detection of the chargino signal necessarily bring in parameters of the chargino decay processes. We simplify our treatment of these processes in the following way: motivated by $\mu \rightarrow e\gamma$ and flavor changing neutral current constraints [20], we assume that all left-handed sleptons of different generations are roughly degenerate (to within, say, 20 GeV) with mass $m_{\tilde{l}}$, and the left-handed squarks of the first two generations are roughly degenerate with mass $m_{\tilde{q}}$. In fact, chargino events are usually insensitive to all other sfermion masses. Decays through third generation squarks are suppressed because, for NLC energies, the mass difference $m_{\tilde{\chi}_1^\pm} - m_{\tilde{\chi}_1^0}$ is almost always less than the top quark mass. For the remaining sfermions, the right-handed sfermion diagrams are suppressed by Higgs couplings m_f/M_W and are negligible.

With these assumptions, there are only six parameters that enter the complete description of chargino pair-production: μ , M_2 , $\tan\beta$, M_1 , $m_{\tilde{l}}$, and $m_{\tilde{q}}$. We do not assume gaugino mass unification, and so M_2 and M_1 are unrelated. With an e_L^- beam, $\tilde{\chi}_1^+ \tilde{\chi}_1^-$ production occurs through the s -channel Z and γ diagrams and the t -channel $\tilde{\nu}_e$ exchange diagram of Fig. 1, and so the left-handed differential cross section is governed by four parameters:

$$\frac{d\sigma_L}{d\cos\theta} (e_L^- e^+ \rightarrow \tilde{\chi}_1^+ \tilde{\chi}_1^-) = \frac{d\sigma_L}{d\cos\theta} (\mu, M_2, \tan\beta, m_{\tilde{l}}) . \quad (5)$$

In the case of an e_R^- beam, the $\tilde{\nu}_e$ diagram is absent, and so the right-handed differential cross section is dependent on only the first three parameters:

$$\frac{d\sigma_R}{d\cos\theta} (e_R^- e^+ \rightarrow \tilde{\chi}_1^+ \tilde{\chi}_1^-) = \frac{d\sigma_R}{d\cos\theta} (\mu, M_2, \tan\beta) . \quad (6)$$

Charginos decay to the LSP either leptonically through W bosons or virtual sleptons,

$$\tilde{\chi}_1^+ \rightarrow (\tilde{\chi}_1^0 W^{+(*)}, \tilde{\ell}^* \nu, \bar{\ell} \tilde{\nu}^*) \rightarrow \tilde{\chi}_1^0 \bar{\ell} \nu , \quad (7)$$

or hadronically through W bosons or virtual squarks,

$$\tilde{\chi}_1^+ \rightarrow (\tilde{\chi}_1^0 W^{+(*)}, \tilde{q}^* q', \bar{q} \tilde{q}'^*) \rightarrow \tilde{\chi}_1^0 \bar{q} q' , \quad (8)$$

and so all six parameters enter the decay process. The lighter chargino may also decay to LSPs through a virtual charged Higgs H^\pm , but this diagram is suppressed by Higgs couplings and is negligible for all but the most extreme choices of parameters. The heavier chargino may decay through complicated cascade decays. However, when $\tilde{\chi}_2^\pm$ production is kinematically accessible, the only information we will use about $\tilde{\chi}_2^\pm$ is its mass, which we will assume may be measured through threshold scans. The analysis will therefore be independent of $\tilde{\chi}_2^\pm$ branching fractions and other observables dependent on the details of the $\tilde{\chi}_2^\pm$ decay.

The chargino masses $m_{\tilde{\chi}_1^\pm}$ and $m_{\tilde{\chi}_2^\pm}$ and the right-handed cross section σ_R depend only on the parameters μ , M_2 , and $\tan\beta$, and these parameters may be used to define regions with qualitatively different behavior. To understand this, note first that, when $M_2 \gg |\mu|$ or $|\mu| \gg M_2$, the following relations hold [21]:

$$m_{\tilde{\chi}_1^\pm} \approx \min\{|\mu|, M_2\} \quad \text{and} \quad m_{\tilde{\chi}_2^\pm} \approx \max\{|\mu|, M_2\} . \quad (9)$$

These relations are in fact approximately valid in most of the available parameter space. The dependence of σ_R on the parameters is more complicated. In Fig. 2 we plot contours of constant σ_R for fixed $\tan\beta$ in the (μ, M_2) plane. The dependence on $\tan\beta$ is fairly weak; we choose the representative value $\tan\beta = 4$ for illustration. Chargino production is inaccessible for $\sqrt{s} = 500 \text{ GeV}$ in the hatched region, and the cross-hatched region is excluded by the current experimental mass limit $m_{\tilde{\chi}_1^\pm} > 45 \text{ GeV}$ [22,23]. This leaves two bands, one on each side of the $\mu = 0$ axis. At the top of each band, where $M_2 \gg |\mu|$, the chargino is Higgsino-like, $\tilde{\chi}_1^\pm \approx \tilde{H}^\pm$, and we see that σ_R is substantial. However as one moves into the region with $M_2 \lesssim |\mu|$, σ_R quickly drops. This may be understood by noting that, because $\sqrt{s} \gg M_Z$, the γ and Z production diagrams may be replaced to a good approximation by diagrams in which the $U(1)$ and $SU(2)$ gauge bosons B and W^3 are exchanged. However, the e_R^- couples only to B , and the \tilde{W}^\pm couples only to W^3 . Thus, in the region with $M_2 \lesssim |\mu|$, where the chargino is dominated by its wino component and $\tilde{\chi}_1^\pm \approx \tilde{W}^\pm$, the cross section σ_R is highly suppressed.

We are now in a position to define characteristic regions in the parameter space. These are shown for $\tan\beta = 4$ in the (μ, M_2) plane in Fig. 3. The hatched and cross-hatched regions are as in Fig. 2. In the remaining area, we define the following three regions, each of which includes a $\mu < 0$ part and a corresponding $\mu > 0$ part that is unlabeled:

Region 1: $m_{\tilde{\chi}_1^\pm} + m_{\tilde{\chi}_2^\pm} < \sqrt{s}$. Here $\tilde{\chi}_1^\pm \tilde{\chi}_2^\mp$ production is possible, and so both chargino masses can be measured.

Region 2 (shaded): $m_{\tilde{\chi}_1^\pm} + m_{\tilde{\chi}_2^\pm} > \sqrt{s}$, and $\sigma_R \lesssim 10 fb$.

Region 3 (shaded): $m_{\tilde{\chi}_1^\pm} + m_{\tilde{\chi}_2^\pm} > \sqrt{s}$, and $\sigma_R \gtrsim 50 fb$.

These three regions almost completely fill the region of parameter space in which chargino pair production is allowed at a 500 GeV e^+e^- collider, leaving only a small region in which the mixing is large and the chargino $\tilde{\chi}_2^\pm$ is just above threshold. In this study, we will ignore this small gap. In the two cases we will study in detail, we will assume $m_{\tilde{\chi}_1^\pm} \approx 172 GeV$. For this value, the measurement of $m_{\tilde{\chi}_1^\pm}$ constrains the parameters to lie on the dashed curves shown in Fig. 3. Then, if $\tilde{\chi}_2^\pm$ is not seen, $\sigma_R < 10 fb$ or $\sigma_R > 70 fb$ for $\tan\beta \geq 4$, and further, for $1 < \tan\beta < 4$, only small areas of the (μ, M_2) plane lie outside regions 1–3. For masses $m_{\tilde{\chi}_1^\pm}$ nearer to threshold, the areas not covered by regions 1–3 are larger. However, this can be compensated by raising the collider center-of-mass energy, which increases the size of region 1.

In region 3, if the ratio M_1/M_2 is fixed, $\tilde{\chi}_1^\pm$ and $\tilde{\chi}_1^0$ become increasingly degenerate as M_2 grows. Charginos then decay to invisible LSPs and very soft jets and leptons. It is therefore difficult to choose a representative point in this region, as even the identification of the chargino signal can be difficult in some areas. More generally, if M_1 and M_2 are unrelated (and, of course, independent of μ), $m_{\tilde{\chi}_1^\pm} - m_{\tilde{\chi}_1^0}$ need not be small, even if the chargino is Higgsino-like. Although it may then be possible to verify SUSY relations in region 3, we will not consider this possibility further. However, we note that the MSSM makes a number of nontrivial predictions for region 3. Since $\tilde{\chi}_1^\pm \approx \tilde{H}^\pm$, the $\tilde{\nu}$ production diagram becomes negligible. The production forward-backward asymmetry is thus approximately zero. In addition, since the chargino is Higgsino-like, it decays predominantly through a virtual W , and so the ratio of hadronic to leptonic decays of the chargino should be equal to the corresponding ratio for W bosons. These characteristic features should distinguish a chargino candidate from new particles of other, non-supersymmetric origin.

IV. A SUPERSYMMETRY TEST IN THE MIXED REGION

We now study a representative point in region 1 in detail. The characteristic property of region 1 is that both chargino eigenstates can be produced, and so both masses are measurable. Thus, in this region, a promising approach will be to test the detailed form of the chargino mass matrix. In particular, notice that the matrix of Eq. (2) contains, in addition to the new parameters M_2 , μ , and $\tan\beta$, a dependence on the W mass. This is no accident. The off-diagonal matrix elements of Eq. (2) result from the $H\tilde{W}\tilde{H}$ vertex. This is related by supersymmetry to the $HW\partial H$ vertex, which is related by gauge invariance to the term which gives mass to the W through the Higgs mechanism. Thus, verification that this parameter of Eq. (2) is indeed equal to M_W would be a quantitative test of supersymmetry. This test is formally independent of the neutralino sector and is therefore applicable to models with gauge singlets.

We now investigate the extent to which we can realistically verify this correspondence at the NLC. In this example, and for the rest of this work, we will assume $\sqrt{s} = 500 GeV$. We will present results for integrated luminosities of 30 and 100 fb^{-1} , corresponding roughly to

$\frac{1}{2}$ to 2 years running at design luminosity.

For our case study, we choose the underlying supersymmetry parameters to be

$$(\mu, M_2, \tan \beta, M_1/M_2, m_{\tilde{t}}, m_{\tilde{q}}) = (-195, 210, 4, 0.5, 400, 700) . \quad (10)$$

For these values, the MSSM gives

$$\begin{aligned} m_{\tilde{\chi}_1^\pm} &= 172 \text{ GeV} \\ m_{\tilde{\chi}_1^0} &= 105 \text{ GeV} \\ m_{\tilde{\chi}_2^\pm} &= 255 \text{ GeV} \\ (\phi_+, \phi_-) &= (40.8^\circ, 59.5^\circ) \\ \sigma_R &= 48 \text{ fb} \\ \sigma_L &= 513 \text{ fb} . \end{aligned} \quad (11)$$

For comparison, the QED $\mu^+\mu^-$ production cross section is 397 fb.

To investigate the expected sensitivity to the form for the chargino mass matrix, we generalize Eq. (2) to an arbitrary real 2×2 matrix, which we parametrize as

$$M'_{\tilde{\chi}^\pm} = \begin{pmatrix} M_2 & \sqrt{2} M_W^X \sin \beta^x \\ \sqrt{2} M_W^X \cos \beta^x & \mu \end{pmatrix} . \quad (12)$$

Without SUSY, the ratio of off-diagonal elements need not be the ratio of vevs $\tan \beta \equiv \langle H_2^0 \rangle / \langle H_1^0 \rangle$, and we have therefore replaced β by β^x . As demanded by gauge invariance, we also replace M_Z by $M_Z^x \equiv M_Z (M_W^x / M_W)$ in the neutralino mass matrix of Eq. (4).¹

We will investigate to what extent the NLC experiments may confirm the SUSY relation $M_W^x = M_W$. More explicitly, we have extended the six-dimensional SUSY parameter space to a seven-dimensional parameter space, and we will investigate how well experiments may reduce the allowed region of this space to the supersymmetric subvolume in which $M_W^x = M_W$. Formally, this is a simple task. The four parameters entering Eq. (12) may be exchanged for the two masses and two mixing angles, $(m_{\tilde{\chi}_1^\pm}, m_{\tilde{\chi}_2^\pm}, \phi_+, \phi_-)$. By determining these four quantities from experiment, we can recover a constraint on M_W^x .

To determine the chargino masses and mixing angles from experiment, we will need to make assumptions about the decay properties of charginos. In our analysis, we will assume that these properties are those of a supersymmetric model at some point in parameter space, with the exception that the new chargino and neutralino mass matrices are used. Because we have not generalized the decay completely, this assumption is a compromise, but we feel, a reasonable one — it gives us a large but well-defined space of possibilities to consider. In addition, we will see below, by explicitly scanning this space, that our results depend only weakly on the decay parameters. The main dependences are kinematic and would be expected in more general models of chargino decays. It is also worth noting that many of our assumptions may be checked a posteriori; for example, the assumption of a universal

¹The resulting neutralino mass matrix is not the most general allowed by gauge invariance. The fully general neutralino mass matrix will be considered briefly when neutralino events are considered in Sec. VI.

left-handed slepton mass may be checked by observing the universality of leptonic branching fractions in chargino decay.

The precision with which $m_{\tilde{\chi}_1^\pm}$ and $m_{\tilde{\chi}_1^0}$ can be determined was studied by the JLC group [6]. Using a method that depends on kinematic arguments only, they found that, for an integrated luminosity of 20 fb^{-1} , these masses could be determined to approximately 2 GeV, an uncertainty that is negligible for this study. The mass $m_{\tilde{\chi}_2^\pm}$ may be determined by scanning near $\tilde{\chi}_1^\pm \tilde{\chi}_2^\mp$ threshold. Although $\sigma(e^+e^- \rightarrow \tilde{\chi}_1^\pm \tilde{\chi}_2^\mp)$ is suppressed by about an order of magnitude from mixing angles, we will assume that an energy scan will be able to determine $m_{\tilde{\chi}_2^\pm}$ to a few GeV, and we will therefore also neglect this uncertainty in the following analysis.

The crucial difficulty will be that of determining the two mixing angles. In principle, these can be extracted by measuring the right-polarized differential cross section for $\tilde{\chi}_1^\pm$ pair production, which is completely determined by the $\tilde{\chi}_1^\pm$ mass and the two mixing angles. The right-polarized cross section σ_R , though an order of magnitude smaller than σ_L , is still large enough to yield a sufficient number of events for precision studies. In particular, we will examine two quantities based on $d\sigma_R/d\cos\theta$: the total cross section σ_R , and a truncated forward-backward asymmetry

$$A_R^X \equiv \frac{\sigma_R(0 < \cos\theta < 0.755) - \sigma_R(-1 < \cos\theta < 0)}{\sigma_R(-1 < \cos\theta < 0.755)}, \quad (13)$$

where θ is defined as the angle between the e^+ beam and the positive chargino $\tilde{\chi}_1^+$. (The motivation for this peculiar definition of A_R^X will be given below.) With $m_{\tilde{\chi}_1^\pm}$ known, the values of σ_R and A_R^X determine the variables (ϕ_+, ϕ_-) and may therefore bound $M_{\tilde{W}}$. This strategy is appealing, because we have seemingly eliminated all dependence on three of the undetermined parameters of the theory: M_1 , $m_{\tilde{t}}$, and $m_{\tilde{q}}$.

Unfortunately, the analysis is not independent of these three parameters when we consider what quantities are actually observable. Cuts must be imposed to reduce standard model backgrounds. In this paper, we will rely on a standard set of cuts which have been previously suggested to isolate the chargino pair production signal. These cuts select chargino events in which one chargino decays to an isolated final state lepton, and the other decays *directly* to hadrons. (Charginos may also decay indirectly to hadrons through τ leptons.) We will call such events “Y mode events,” with the letter “Y” chosen to suggest the typical $2j + \ell$ topology of these events. What is actually measured is not σ_R , but the Y mode partial cross section after cuts,

$$\eta\sigma_Y \equiv 2\eta B_\ell B_h \sigma_R, \quad (14)$$

where η is the efficiency of the cuts for Y events, B_h is the chargino branching ratio for direct hadronic decays, and B_ℓ is the branching ratio for decays to a final-state lepton. These fractions both exclude decays to a τ which subsequently decays hadronically.

Since the charginos decay very quickly, with typical widths of 1–100 keV, the chargino direction and the asymmetry A_R^X cannot be determined directly. We will measure A_R^X through its correlation to A^{had} , the forward-backward asymmetry of the hadronic system in Y events. In principle, the experimentally observable quantities A^{had} and $\eta\sigma_Y$ depend on the decay distributions, and thus reintroduce dependence on the parameters M_1 , $m_{\tilde{t}}$, and $m_{\tilde{q}}$. To

understand the extent of this problem, we have performed Monte Carlo simulations at a number of points in parameter space. These points have been chosen randomly, subject only to the constraints that they give values of $m_{\tilde{\chi}_1^\pm}$, $m_{\tilde{\chi}_1^0}$, and $m_{\tilde{\chi}_2^\pm}$ consistent with those that would be measured in our case study. We will show below that, in the resulting subvolume of parameter space, the experimental observables turn out to be rather insensitive to M_1 , $m_{\tilde{t}}$, and $m_{\tilde{q}}$, and therefore the virtues of our strategy in fact remain.

To simulate chargino events, we used the parton level Monte Carlo event generator of Ref. [16]. This generator includes the spin correlations between production and decay processes. To simulate hadronization and detector effects, the final state partons were smeared with detector parameters as chosen in the JLC study [6]:

$$\frac{\sigma_E^{had}}{E} = \frac{40\%}{\sqrt{E}} \quad \text{and} \quad \frac{\sigma_E^{lepton}}{E} = \frac{15\%}{\sqrt{E}}, \quad (15)$$

where E is in GeV.

The Y chargino events were selected by first using a system of cuts presented in Ref. [10]. These cuts are designed for charginos that decay through off-shell W bosons, and include the following:

- (a) $|\cos \theta_i| < 0.9$ for every final state parton, where θ_i is the polar angle of parton i with respect to the e^+ beam axis.
- (b) $E_\ell > 5 \text{ GeV}$, $\theta_{q\ell} > 30^\circ$, that is, there must be an energetic e or μ with no hadronic activity within a cone of half angle 30° .
- (c) $20 \text{ GeV} < E_{visible} < \sqrt{s} - 100 \text{ GeV}$.
- (d) $\theta_{acoplanarity} < 150^\circ$.
- (e) $m_{had} < 68 \text{ GeV}$, $E_{had} < \sqrt{s} - 100 \text{ GeV}$, where m_{had} and E_{had} are the mass and energy of the hadronic system.
- (f) $|m_{\ell\nu} - M_W| > 10 \text{ GeV}$, where the ν momentum is taken to be equal to the missing momentum.
- (g) $-Q_\ell \cos \theta_{had}, Q_\ell \cos \theta_\ell < \cos 41^\circ = 0.755$, where Q_ℓ is the charge of the isolated lepton, and θ_i is as defined in cut (a).

These cuts isolate chargino events that have hadrons and an isolated lepton in the final state. We would like to isolate Y events, and we therefore need to eliminate events in which the hadronic system results from charginos decaying through τ leptons. This may be done by imposing the additional requirement that the mass of the hadronic system m_{had} be greater than m_τ . As was shown in Ref. [16], Y events very rarely have low m_{had} at LEP II energies, and we have verified that this is also true for NLC energies. We will therefore simply assume that this additional cut on m_{had} cleanly isolates the Y mode events.

Cuts (c) and (d) are efficient for supersymmetric signals because of the large momentum and energy that are carried off by the unobserved massive LSPs. Cuts (e)–(g) reduce the dominant standard model background, W pair production. In particular, cut (g) is designed to remove the large forward peak of WW events. Because the hadronic system's polar angle distribution is truncated by cut (g), we choose A_R^X , as defined in Eq. (13), as the theoretical quantity with which we expect A^{had} to be well-correlated. Since W pair production results primarily from e^-e^+ annihilation, the use of these cuts in conjunction with a very highly right-polarized e^- beam results in a negligible background rate. The analysis of Ref. [10]

included $t\bar{t}$ events with a top quark mass of 150 GeV and found negligible background from this source.

We caution the reader that the cuts (a)–(g) above have been designed to separate the chargino signal from standard model backgrounds, but have not been optimized to discriminate between $\tilde{\chi}_1^+ \tilde{\chi}_1^-$ production and other SUSY sources of Y events. In principle, these could include $\tilde{\chi}_1^\pm \tilde{\chi}_2^\mp$ and $\tilde{\chi}_2^+ \tilde{\chi}_2^-$ production, as well as the production of neutralino pairs $\tilde{\chi}_i^0 \tilde{\chi}_j^0$. Ignoring effects of resolution smearing, the neutralino events will be backgrounds to Y events only when a heavy neutralino decays into a chargino and a W boson, which then decays leptonically to provide the single isolated lepton. While we have not simulated these events, we do not expect neutralinos to be a severe background because their production cross sections are generally small, and further, their decays to $h\tilde{\chi}_1^0$ and $Z\tilde{\chi}_1^0$ are usually favored by phase space and therefore dominate. For the point that we are studying, the masses of the heavy neutralinos are $m_{\tilde{\chi}_2^0} = 169 \text{ GeV}$, $m_{\tilde{\chi}_3^0} = 211 \text{ GeV}$, and $m_{\tilde{\chi}_4^0} = 253 \text{ GeV}$. The decay $\tilde{\chi}_4^0 \rightarrow W\tilde{\chi}_1^\pm$ is barely open, and the production of heavy chargino pairs is kinematically forbidden. Thus, $\tilde{\chi}_1^\pm \tilde{\chi}_2^\mp$ production, with $\tilde{\chi}_2^\pm \rightarrow W^\pm \tilde{\chi}_1^0 \rightarrow \ell^\pm \nu \tilde{\chi}_1^0$ is the main SUSY contamination in the present case study. This background is restricted by phase space and mixing angles and can be eliminated entirely by running below the $\tilde{\chi}_1^\pm \tilde{\chi}_2^\mp$ production threshold.

Throughout this study, we have assumed 100% beam polarization in our simulations. In the present case, however, because σ_L is an order of magnitude larger than σ_R , the left-handed contamination of the right-handed beam could be substantial if the beam polarization is not nearly 100%. If beam polarization near 100% is unobtainable, the e_R^- signal may be determined by first measuring the e_L^- signal to high accuracy, and then subtracting the left-handed contamination from the right-polarized e^- beam's signal. For a beam polarization of 95%, these errors will not be large, and we have not included the statistical errors resulting from such a subtraction. It is clear, however, that highly polarized beams play a critical role in reducing such errors.

We now determine the correlation of A_R^X with A^{had} through Monte Carlo simulations. A description of our method and the relevant formulae are contained in the appendix. We sample random points in the seven dimensional parameter space, with only the restriction that $m_{\tilde{\chi}_1^\pm}$, $m_{\tilde{\chi}_1^0}$, and $m_{\tilde{\chi}_2^\pm}$ are each within 2 GeV of their values in Eq. (11). For each set of parameters, we calculate A_R^X from explicit analytical formulae and determine A^{had} through Monte Carlo simulation. The results for 38 simulations are plotted in Fig. 4. A simple linear fit yields $A^{had} = 0.717A_R^X + 0.042 \pm 0.036$, where $\Delta A_{MC}^{tot} = 0.036$ is the 1σ deviation in A^{had} for a fixed A_R^X . The best fit is given by the solid line in Fig. 4, and the 1σ deviations are shown by the dashed lines.

However, this quoted error overestimates the deviation from perfect correlation between A_R^X and A^{had} , because each point in Fig. 4 was computed from a finite sample of Monte Carlo events and therefore contains a non-negligible statistical fluctuation. The average effective number of Monte Carlo events for the simulations was $N_{MC} \approx 1400$. Using the formulae contained in the appendix, we find that the Monte Carlo statistical error is $\Delta A_{MC}^{stat} = 0.026$; when this is removed, the systematic error in assuming perfect correlation is found to be $\Delta A^{sys} = 0.025$. The correlation between A_R^X and A^{had} is high — the chargino rest frames are slightly boosted, and the decay distributions are sufficiently similar for all sampled values of the underlying parameters that A^{had} is highly insensitive to the decay process and is well-determined for a fixed A_R^X . (If the beam energy is slightly reduced to run below

the $\tilde{\chi}_1^\pm \tilde{\chi}_2^\mp$ threshold, the charginos will be less boosted. However, we do not expect the correlation between A_R^X and A^{had} to deteriorate much, since, even in the present case with $\sqrt{s} = 500 \text{ GeV}$ and only slightly boosted charginos, the correlation is high.)

To determine the bounds that may be placed on A_R^X experimentally, we must add the experimental statistical error to ΔA^{sys} . For our representative point, a Monte Carlo simulation gives

$$\begin{aligned} A^{had} &= -0.233 \\ \eta &= 35.5\% \\ N_{exp} &= 6.0 \mathcal{L}_R, \end{aligned} \tag{16}$$

where N_{exp} is the number of Y events surviving the cuts, and \mathcal{L}_R is the right-handed integrated luminosity in fb^{-1} . The total experimental uncertainties for two values of right-polarized integrated luminosity are found to be

$$\mathcal{L}_R = 30 (100) \text{ fb}^{-1} \implies A_R^X = -0.37 \pm 0.107 (0.065). \tag{17}$$

The efficiency η also depends on the decay process. We determine η by finding its range in the subvolume of parameter space in which the three masses and A_R^X are within the experimental bounds of their underlying values. Each simulation gives a point in the (A_R^X, η) plane, and the distribution of points is plotted in Fig. 5. A linear fit gives $\eta = -6.48 A_R^X + 34.35 \pm 1.07\%$, where $\Delta \eta_{MC}^{tot} = 1.07\%$ is the 1σ deviation in η for a fixed A_R^X . As in the previous figure, the best linear fit is given by the solid line, and the dashed lines give the 1σ deviations. We see that there is a dependence on A_R^X — in cases in which chargino production is forward peaked, cut (g) lowers the efficiency. However, since we have already bounded A_R^X in the analysis above, we may use this measurement to restrict the range of η . To determine the systematic error, we remove the Monte Carlo statistical error from $\Delta \eta_{MC}^{tot}$. Following the analysis of the appendix, we find that $\Delta \eta_{MC}^{stat} = 0.77\%$ and $\Delta \eta^{sys} = 0.75\%$, and, including experimental statistical errors, we find

$$\mathcal{L}_R = 30 (100) \text{ fb}^{-1} \implies \frac{\Delta \sigma_Y}{\sigma_Y} = 8.0 (4.7)\%. \tag{18}$$

To convert a measurement of σ_Y into a measurement of σ_R , we must also take into account the uncertainty in the branching ratios B_l and B_h . These again depend on the parameters of the chargino decay matrix elements and, in particular, on the masses $m_{\tilde{t}}$ and $m_{\tilde{q}}$. We have varied these masses to permit as large a variation in σ_R as possible. However, the measurements of $m_{\tilde{\chi}_1^\pm}$, $m_{\tilde{\chi}_2^\pm}$, A_R^X , and σ_Y constrain the allowed parameter ranges to regions where $\tilde{\chi}_1^+$ and $\tilde{\chi}_1^-$ have substantial Higgsino components. Recall that B_l and B_h take fixed values (equal to those for the W) in the Higgsino limit. These facts and the bounds $m_{\tilde{t}}, m_{\tilde{q}} > 250 \text{ GeV}$ constrain the Y mode branching fraction to the region in which $29\% < 2B_l B_h < 36\%$. Thus, the σ_Y contours are rather insensitive to variations in the sfermion mass parameters.

The measurements of A_R^X and σ_R constrain the (ϕ_+, ϕ_-) plane to the shaded regions in Fig. 6. The lightly (heavily) shaded region is the allowed region for $\mathcal{L}_R = 30 (100) \text{ fb}^{-1}$. Contours of constant $M_{\tilde{W}}^X$ are also plotted in GeV, with the SUSY contour $M_{\tilde{W}}^X = M_W$ given by the dotted curves. The contours of constant σ_R that bound the allowed region run

roughly northwest to southeast; contours of constant A_R^X run roughly southwest to northeast. The indicated boundaries correspond to 1σ deviations in each quantity.

Given the chargino masses of this case study, the theoretically possible range of M_W^X is

$$0 \leq M_W^X \leq \left(\frac{m_{\tilde{\chi}_1^\pm}^2 + m_{\tilde{\chi}_2^\pm}^2}{2} \right)^{\frac{1}{2}} = 218 \text{ GeV} . \quad (19)$$

In the allowed region for $\mathcal{L}_R = 100 \text{ fb}^{-1}$,

$$60 \text{ GeV} < M_W^X < 105 \text{ GeV} . \quad (20)$$

The measurement of M_W^X , therefore, provides a quantitative confirmation of SUSY.

As an aside, we note that our analysis simultaneously bounds the parameters μ , M_2 , and $\tan \beta^X$. In the heavily shaded region, the allowed ranges for these parameters are

$$\begin{aligned} -204 \text{ GeV} &< \mu < -183 \text{ GeV} \\ 199 \text{ GeV} &< M_2 < 217 \text{ GeV} \\ 2.4 &< \tan \beta^X . \end{aligned} \quad (21)$$

If one is led by the bounds on M_W^X (or other considerations) to view SUSY and the MSSM as confirmed, one might then consider only the contour $M_W^X = M_W$ within the allowed region. One would also be led to identify $\tan \beta^X$ with the ratio of Higgs scalar vevs, and so we will replace β^X with β . On the contour $M_W^X = M_W$, the bounds on the SUSY parameters are extremely strong:

$$\begin{aligned} -196 \text{ GeV} &< \mu < -193 \text{ GeV} \\ 208 \text{ GeV} &< M_2 < 211 \text{ GeV} \\ 3.9 &< \tan \beta < 4.1 . \end{aligned} \quad (22)$$

These bounds are so strong that it is likely that the uncertainties in chargino masses will be a significant source of uncertainty. (Recall that, while the uncertainties in chargino masses were included in the determination of systematic errors, the parameter bounds are determined from Fig. 6, in which the chargino masses are fixed.) Nevertheless, it is clear that the discovery of both chargino mass eigenstates will allow one to place tight bounds on these three central SUSY parameters. In particular, the bound on $\tan \beta$ would be one of the most stringent and model-independent; the difficulty of determining $\tan \beta$ from the Higgs scalar sector is explained in Ref. [24]. Given the bounds of Eq. (22), other SUSY parameters may be restricted by additional measurements. For example, $m_{\tilde{\chi}_1^0}$ may be used to determine M_1 , and σ_L may be used to find $m_{\tilde{t}}$. Such determinations may help lead us to an understanding of the SUSY breaking mechanism and other aspects of higher theories.

We have now completed the case study for our chosen representative point. We conclude this section with comments concerning the power of this analysis for other points in region 1. If one moves from the point given in Eq. (10) toward region 3, the results of the analysis become stronger for two reasons. First, σ_R increases, and the experimental statistical errors decrease. Second, as a direct consequence of electroweak gauge invariance, such large values of σ_R can only be achieved for Higgsino-like $\tilde{\chi}_1^\pm$, even in the generalized (seven-dimensional) parameter space where one lets M_W^X vary. This implies that chargino decay is dominated by

the W diagram, and the sensitivity to the decay process parameters becomes even weaker than in our case study. In particular, the systematic errors related to determining A_R^X and η become smaller, and the branching ratios B_l and B_h take their W decay values.

If one moves in the opposite direction toward region 2, the number of right-polarized events deteriorates rapidly. In addition, $\tilde{\chi}_1^\pm$ may be gaugino-like, and the branching fractions therefore depend more strongly on decay parameters, leading to a larger uncertainty in the determination of σ_R from σ_Y . These problems can potentially be remedied by changing the analysis method. Since a highly right-polarized e^- beam leads to a very small level of background, it may be possible to use a looser system of cuts, and to measure the hadronic and leptonic branching fractions directly. The analysis in the gaugino-like portion of region 1 would then be limited only by statistics and systematic errors in the determination of A_R^X and η , and the statistical uncertainties in the measurements of the branching fractions for chargino decays.

Finally, having considered variations of the Higgsino-gaugino content of $\tilde{\chi}_1^\pm$, one might consider variations orthogonal to these in the plane of Fig. 3, namely, variations in $m_{\tilde{\chi}_1^\pm}$. If $\tilde{\chi}_1^\pm$ is heavier, the chargino rest frame is less boosted relative to the lab frame. The decay process will then have a bigger effect on the correlation of A^{had} with A_R^X , and ΔA^{sys} will increase. However, we have already considered a case with a fairly heavy $\tilde{\chi}_1^\pm$, and we see that the charginos need not be highly relativistic for ΔA^{sys} to be small. In the opposite limit of lighter $\tilde{\chi}_1^\pm$, the chargino rest frame is more boosted relative to the lab frame, decay effects become less important, and the results of our analysis can be expected to improve.

V. A SUPERSYMMETRY TEST IN THE GAUGINO REGION

In the previous section, we considered the case in which both charginos were discovered, and found that the SUSY constraint on the chargino mass matrix could be verified to fairly high precision. In this section, we examine region 2, in which only one chargino is seen and its production cross section from e_R^- is small. Here we must rely on the chargino pair production cross section from e_L^- , which introduces a strong dependence on $m_{\tilde{\nu}}$ from the second diagram in Fig. 1. Fortunately, there is an important compensating simplification: in this region, the charginos are very nearly pure gauginos, and, in fact, it is a good approximation to neglect the deviations of $\cos \phi_\pm$ from 1. In this limit, the coupling constant of the $e^\mp \tilde{\nu} \tilde{\chi}_1^\pm$ vertex is related by supersymmetry to the $e^\mp \nu W^\pm$ coupling constant g . Verification that this coupling constant is indeed equal to g would be a quantitative test of supersymmetry.

For our case study in region 2, we take the underlying supersymmetry parameters to be

$$(\mu, M_2, \tan \beta, M_1/M_2, m_{\tilde{\nu}}, m_{\tilde{g}}) = (-500, 170, 4, 0.5, 400, 700) . \quad (23)$$

For these values, the MSSM gives

$$\begin{aligned}
m_{\tilde{\chi}_1^\pm} &= 172 \text{ GeV} \\
m_{\tilde{\chi}_1^0} &= 86 \text{ GeV} \\
m_{\tilde{\chi}_2^\pm} &= 512 \text{ GeV} \\
(\phi_+, \phi_-) &= (1.2^\circ, 12.8^\circ) \\
\sigma_R &= 0.15 \text{ fb} \\
\sigma_L &= 612 \text{ fb} .
\end{aligned} \tag{24}$$

For the point we have chosen (and for a significant part of region 2), the two-body chargino decay $\tilde{\chi}_1^\pm \rightarrow W^\pm \tilde{\chi}_1^0$ is open. The branching fractions B_ℓ and B_h are then fixed to their values in W decay, unless $|\mu|$ is very large, a possibility discussed at the end of this section. The case in which on-shell W decays are not allowed will also be discussed briefly at that point.

To investigate the sensitivity of experiments to the value of the $e^\mp \tilde{\nu} \tilde{\chi}_1^\pm$ coupling, we generalize this coupling from its SUSY value gV_{11} to $g^x V_{11}$. We then test the SUSY relation $g^x = g$. The differential cross section $d\sigma_L/d\cos\theta$ is then a function of $(m_{\tilde{\chi}_1^\pm}, \phi_+, \phi_-, m_{\tilde{\nu}}, g^x)$, but because $\phi_+, \phi_- \approx 0$ and we can measure $m_{\tilde{\chi}_1^\pm}$, we have only two unknowns. These may be constrained with two quantities formed from $d\sigma_L/d\cos\theta$, which we choose to be σ_L and

$$A_L^x \equiv \frac{\sigma_L(0 < \cos\theta < 0.707) - \sigma_L(-1 < \cos\theta < 0)}{\sigma_L(-1 < \cos\theta < 0.707)} . \tag{25}$$

It is important to note that the parameters g^x and $m_{\tilde{\nu}}$ enter $d\sigma_L/d\cos\theta$ only through the $\tilde{\nu}$ diagram amplitude, which has the form

$$A_{\tilde{\nu}} \sim \frac{|g^x V_{11}|^2}{t - m_{\tilde{\nu}}^2} . \tag{26}$$

Thus, for very large values of $m_{\tilde{\nu}}$, only the ratio $g^x/m_{\tilde{\nu}}$ can be determined. However, we will see that even for the rather large value of $m_{\tilde{\nu}}$ that we have chosen, the two parameters g^x and $m_{\tilde{\nu}}$ can be distinguished. In general, these parameters can be bounded independently when $m_{\tilde{\nu}}$ is comparable to the collider center-of-mass energy (though still possibly above the pair-production threshold).

We follow the procedure of the previous section, with the exception of using the cuts of Ref. [25], which are appropriate for charginos decaying through on-shell W bosons. These include the following:

- (a) $E_\ell > 5 \text{ GeV}$, $\theta_{q\ell} > 60^\circ$.
- (b) $\cancel{E}_T > 35 \text{ GeV}$.
- (c) $\theta_{\text{acoplanarity}} < 150^\circ$.
- (d) $|m_{\ell\nu_{ISR}} - M_W| > 10 \text{ GeV}$, where ν_{ISR} is defined to be the massless particle which, along with an initial state radiated photon in the $\pm\hat{z}$ direction, makes up the missing momentum.
- (e) $\theta_{\text{sphericity}} < 45^\circ$, which we approximate in the Monte Carlo simulation by demanding $-Q_\ell \cos\theta_{\text{had}}, Q_\ell \cos\theta_\ell < \cos 45^\circ = 0.707$.

This system of cuts isolates chargino events containing hadrons and an isolated lepton. Again, the subset of these events that are Y mode events may be cleanly separated by demanding that m_{had} be significantly larger than m_τ . After these cuts, the WW background is reduced to roughly 25 fb for an e_L^- beam, which is approximately the size of the signal after cuts. We will assume that the WW background is well-understood and may be subtracted

up to statistical fluctuations. As the WW background is strongly forward-peaked, we will also assume in computing statistical errors that it contributes completely to the set of events with $\cos\theta > 0$. The $t\bar{t}$ background, computed with $m_t = 140 \text{ GeV}$, is again negligible. In the gaugino region, the other SUSY signals do not provide a significant background to Y events, because the only kinematically accessible SUSY backgrounds are $\tilde{\chi}_2^0\tilde{\chi}_1^0$ and $\tilde{\chi}_2^0\tilde{\chi}_2^0$, with $m_{\tilde{\chi}_2^0} \approx m_{\tilde{\chi}_1^\pm}$. The neutralinos $\tilde{\chi}_2^0$ then decay to LSPs and an even number of leptons, and the number of events with one isolated lepton is highly suppressed.

To determine the correlation between A^{had} and A_L^X , we perform Monte Carlo simulations at a number of randomly chosen points in the seven-dimensional parameter space $(\mu, M_2, \tan\beta, M_1/M_2, m_{\tilde{L}}, m_{\tilde{Q}}, g^X)$, subject to the constraints that $m_{\tilde{\chi}_1^\pm}$ and $m_{\tilde{\chi}_1^0}$ are within 2 GeV of their measured values and $\sigma_R < 1 \text{ fb}$. Again the experimental observable A^{had} is determined to be an excellent estimator of A_L^X , with $\Delta A^{sys} = 0.034$. A Monte Carlo simulation at our representative point gives

$$\begin{aligned} A^{had} &= 0.034 \\ \eta &= 11.9\% \\ N_{exp} &= 25.8\mathcal{L}_L, \end{aligned} \tag{27}$$

where \mathcal{L}_L is the left-handed integrated luminosity in fb^{-1} . We now calculate the uncertainties in determining A_L^X and σ_Y using the equations found in the appendix, this time including also the errors arising from a substantial number of background events $N_{back} \approx N_{exp}$. We find that for two values of left-polarized integrated luminosity,

$$\mathcal{L}_L = 30 (100) \text{ fb}^{-1} \implies A_L^X = 0.20 \pm 0.067 (0.048). \tag{28}$$

As in the previous case, the efficiency η is found to be highly constrained by the measurements of $m_{\tilde{\chi}_1^\pm}$, $m_{\tilde{\chi}_1^0}$, σ_L , and A_L^X , and the resulting systematic error is $\Delta\eta^{sys} = 0.55\%$. Including experimental statistical errors and those resulting from background subtraction, we find

$$\mathcal{L}_L = 30 (100) \text{ fb}^{-1} \implies \frac{\Delta\sigma_Y}{\sigma_Y} = 7.2 (5.6) \%. \tag{29}$$

For $\mathcal{L}_L = 30$ and 100 fb^{-1} these measurements constrain the allowed region of the $(m_{\tilde{\nu}}, g^X)$ plane to the shaded areas shown in Fig. 7. Because the charginos decay through on-shell W bosons, in contrast to the region 1 analysis, B_t and B_h are fixed at their values in W decay, and thus the contours for σ_L inferred from σ_Y are independent of sfermion masses. For $\mathcal{L}_L = 100 \text{ fb}^{-1}$, if $m_{\tilde{\nu}} < 250 \text{ GeV}$ is excluded by the non-observation of any other threshold for heavy particle production, the allowed region is only the largest of the three shaded regions in Fig. 7b. For this region, we find the constraint

$$0.85g \leq g^X \leq 1.3g. \tag{30}$$

Such a result would be an important quantitative confirmation of SUSY.

Fig. 7 also illustrates a number of other interesting features. It is clear from Fig. 7 that, without assuming SUSY, the analysis above has simultaneously bounded the mass $m_{\tilde{\nu}}$ of a t -channel resonance, a useful result for future particle searches. If, on the other hand, we

assume the validity of SUSY, then we are restricted to the dotted line at $g^x/g = 1$, and the A_L^x measurement *alone* restricts $m_{\tilde{\nu}}$. Alternatively, the σ_L measurement *alone* restricts $m_{\tilde{\nu}}$ to two different ranges, of which one can be immediately excluded. Finally, as expected from earlier comments, this analysis is significantly weakened if $m_{\tilde{\nu}}$ is large. For large $m_{\tilde{\nu}}$, the contours of Fig. 7 approach contours of constant $g^x/m_{\tilde{\nu}}$, and only the ratio $g^x/m_{\tilde{\nu}}$ can be determined. On the other hand, if it is possible to measure $m_{\tilde{\nu}}$ independently, for example, from $e^{\mp}\tilde{\nu}\tilde{\chi}_1^{\pm}$ production, then the bounds on g^x/g can be significantly improved.

In the example above, we have considered a point for which chargino decays through on-shell W bosons are allowed. This choice was motivated by two considerations. First, in region 1, we considered a point for which only off-shell W decays were possible, and appropriate cuts were used. Our choice in region 2 illustrates that tests of SUSY are also possible when cuts appropriate to on-shell W decays must be used. Second, the scenario in which on-shell W decays are possible becomes more and more typical as the chargino mass rises, and the analysis presented is thus generalizable to higher chargino masses and beam energies. It is easy, however, to find points in region 2 where the chargino cannot decay to an on-shell W . For example, if one assumes the GUT relation $M_2 = 2M_1$, on-shell W decays are excluded for $m_{\tilde{\chi}_1^{\pm}} \lesssim 160 \text{ GeV}$. In this case, we must use the cuts presented in Sec. IV. In addition, chargino decays through virtual sfermions are not negligible, and one must consider the dependences of the branching ratios on sfermion masses. Such dependences will introduce systematic errors that may considerably weaken our results. However, as in the case of the gaugino portion of region 1, if these branching ratios can be measured, the systematic errors in their determination may be greatly reduced. In contrast to the region 1 case, the e_L^- beam, with its accompanying WW background, must be used. However, because WW events do not usually have \cancel{e}_T without isolated leptons, they are likely to be a small background to purely hadronic chargino events. Although further study is required, it again seems probable that the Y mode branching fraction can be measured directly, and, with these modifications, the previous analysis may be applied to region 2 scenarios in which only off-shell W decays are allowed.

It is also true that in the very far gaugino region with $|\mu| \gg M_2$, where $\tilde{\chi}_1^{\pm} \approx \tilde{W}^{\pm}$ and $\tilde{\chi}_1^0 \approx \tilde{B}$, the W decay diagram is suppressed by mixing angles, and, even when decays through on-shell W bosons are kinematically allowed, virtual sfermion diagrams may be important. This requires that $\tilde{\chi}_1^{\pm}$ and $\tilde{\chi}_1^0$ be very nearly pure gauginos, however, and this occurs only for $|\mu| \gtrsim 1 \text{ TeV}$, a condition that is disfavored by fine-tuning constraints.

VI. SFERMIONS AND NEUTRALINOS

Up to this point, we have considered only precision SUSY tests from studies of the properties of charginos. Other sparticles may be produced at NLC energies, however, and we now examine the possibility of testing SUSY through the properties of sfermions and neutralinos. The discussion will be limited to brief remarks and, in contrast to the previous sections, no attempt will be made to perform detailed studies.

We first investigate the possibility of identifying a few newly-discovered scalars as sfermions. We are most interested in the scenario in which these scalars provide the first opportunity for precision tests of SUSY, and we therefore consider the case in which these scalars are lighter than charginos. In contrast to the previous sections, we will not impose

any constraints on intergenerational slepton and squark mass degeneracies. However, if the problem is considered in full generality, it is complicated by many arbitrary parameters associated with sfermion intergenerational mixing. Simply to make the problem tractable, we will assume that intergenerational mixing is absent. We will also assume that left-right mixings may be neglected, with the understanding that the discussion that follows may not be applicable to the sfermions of the third generation. Probes of the left-right mixing of scalar taus have recently been discussed by Nojiri [26].

With these assumptions, the properties of these sfermions are completely specified by their quantum numbers and their masses. The only category (III) tests involving sfermion properties are therefore verifications of mass relations. Given the assumptions above, the masses of sfermions are

$$\begin{aligned}
m_{\tilde{u}_L}^2 &= m_{\tilde{Q}}^2 + m_u^2 + M_Z^2 \left(\frac{1}{2} - \frac{2}{3} \sin^2 \theta_W \right) \cos 2\beta \\
m_{\tilde{d}_L}^2 &= m_{\tilde{Q}}^2 + m_d^2 + M_Z^2 \left(-\frac{1}{2} + \frac{1}{3} \sin^2 \theta_W \right) \cos 2\beta \\
m_{\tilde{u}_R}^2 &= m_{\tilde{U}}^2 + m_u^2 + M_Z^2 \left(\frac{2}{3} \sin^2 \theta_W \right) \cos 2\beta \\
m_{\tilde{d}_R}^2 &= m_{\tilde{D}}^2 + m_d^2 + M_Z^2 \left(-\frac{1}{3} \sin^2 \theta_W \right) \cos 2\beta \\
m_{\tilde{e}_L}^2 &= m_{\tilde{L}}^2 + m_e^2 + M_Z^2 \left(-\frac{1}{2} + \sin^2 \theta_W \right) \cos 2\beta \\
m_{\tilde{\nu}_L}^2 &= m_{\tilde{L}}^2 + \frac{1}{2} M_Z^2 \cos 2\beta \\
m_{\tilde{e}_R}^2 &= m_{\tilde{E}}^2 + m_e^2 + M_Z^2 \left(-\sin^2 \theta_W \right) \cos 2\beta ,
\end{aligned} \tag{31}$$

where $m_{\tilde{Q}}$, $m_{\tilde{U}}$, $m_{\tilde{D}}$, $m_{\tilde{L}}$, and $m_{\tilde{E}}$ are soft SUSY breaking scalar masses. Similar relations hold for second and third generation sfermions. With additional relations from grand unification, there are a number of relations among these scalar masses [2]. However, we will continue to eschew assumptions that are not phenomenologically motivated. Without GUT assumptions, the right-handed masses are unrelated to the other masses, and the left-handed masses are related only by

$$\begin{aligned}
m_{\tilde{e}_L}^2 - m_{\tilde{\nu}_L}^2 &= -M_W^2 \cos 2\beta \\
m_{\tilde{d}_L}^2 - m_{\tilde{u}_L}^2 &= -M_W^2 \cos 2\beta ,
\end{aligned} \tag{32}$$

where we have omitted the small fermion mass terms. For $\tan \beta > 1$, these mass differences are positive, but we will consider all possible values of $\tan \beta$ below. The relations of Eq. (32) are quantitative predictions of SUSY that we may try to test.

Unfortunately, if the newly discovered scalars are sleptons, it will be impossible to test these relations, because the sneutrinos will decay invisibly through $\tilde{\nu}_L \rightarrow \nu \tilde{\chi}_1^0$. We are assuming that charginos are heavier than sneutrinos, and so the decay $\tilde{\nu} \rightarrow e_L \tilde{\chi}_1^+$ is excluded. Also, even if $\tan \beta < 1$ and $m_{\tilde{\nu}_L} > m_{\tilde{e}_L}$, the experimental lower bound $m_{\tilde{e}_L} > 45 \text{ GeV}$ [22,23] implies $m_{\tilde{\nu}_L} - m_{\tilde{e}_L} < 47 \text{ GeV}$, and the decay $\tilde{\nu}_L \rightarrow \tilde{e}_L W^+$ is also greatly suppressed. The masses of sleptons are therefore highly unlikely to provide the *first* category (III) verifications of SUSY. Of course, if sneutrinos are heavier than charginos, precise verifications of slepton mass relations could be used to supplement measurements of chargino properties. It should also be noted that other properties of slepton *events* may provide additional precision measurements in the gaugino region. It may be possible, for example, to measure some neutralino properties through the t -channel $\tilde{\chi}_i^0$ exchange diagrams for charged slepton pair production [10].

On the other hand, if the scalars are squarks, both left-handed species will decay visibly. A previous study of squark mass determination found that at the NLC, in most regions

of parameter space, squark masses can be measured to approximately 2 GeV with an integrated luminosity of $10 fb^{-1}$, even in scenarios with cascade decays [14]. This study also found that left-handed squarks can be effectively separated from right-handed squarks using beam polarization. It may be difficult to properly assign flavors to the different squark mass thresholds, however, especially if these thresholds are not well-separated. Let us first suppose that the masses of only two left-handed squarks are determined. To verify SUSY quantitatively, one must assume that the squarks are in the same generation, and must also independently determine $\tan\beta$ from the Higgs scalar sector. This is by no means always possible, and most likely requires, for example, that $m_{A^0} \lesssim 300 GeV$ so that a heavy Higgs boson is kinematically accessible [24]. Even if all of these measurements can be made, the precision of the test is not high. For example, if $m_{\tilde{q}} > 200 GeV$, the mass difference is $|m_{\tilde{u}_L} - m_{\tilde{d}_L}| < 15 GeV$, and so in the best case scenario where $\tan\beta$ is determined exactly, the squark mass relation can be verified to approximately 20%. If it is not possible to measure $\tan\beta$ from the Higgs boson sector, a precision test of squark mass relations is only possible if one measures four left-handed squark masses. One can then check that there exists some flavor assignment consistent with

$$m_{\tilde{d}_L}^2 - m_{\tilde{u}_L}^2 \approx m_{\tilde{s}_L}^2 - m_{\tilde{c}_L}^2 \equiv \Delta(m^2), \quad (33)$$

where $|\Delta(m^2)| \leq M_W^2$.

The possibility of making the first quantitative tests of SUSY from sfermion properties is therefore not very promising. In the case of sleptons, the prospects are bleak, while in the case of squarks, even after assuming that intergenerational mixing is absent, precision tests are complicated by difficulties in flavor determination and rely on many MSSM scalars being kinematically accessible. However, the sfermion sector provides a number of opportunities for disproving the MSSM and SUSY. For example, if sneutrino decay is observed, one of our assumptions must be invalid. Also, the relations of Eq. (32) are valid not just for the MSSM, but are extremely general predictions of SUSY. If they are found to be violated, not only will the MSSM be excluded, but almost all supersymmetric models will be strongly disfavored. On the other hand, if SUSY is favored by experiment, measurements of the squark and slepton masses will give important information about the flavor dependence of the SUSY breaking mechanism.

Neutralinos are natural candidates for precision SUSY tests, because, with the assumption that the lightest neutralino $\tilde{\chi}_1^0$ is the LSP, all sparticle event observables depend, at least formally, on the parameters that determine neutralino properties. In addition, neutralinos are light in many models, and, in fact, throughout parameter space, if charginos are produced, $\tilde{\chi}_1^0 \tilde{\chi}_2^0$ production is kinematically possible.

One might hope to follow the procedure in Sec. IV by generalizing the neutralino mass matrix. If we relax SUSY, the most general form of Eq. (4) consistent with gauge invariance is

$$M'_{\tilde{\chi}^0} = \begin{pmatrix} M_1 & 0 & & \\ & 0 & M_2 & \mathcal{M} \\ & \mathcal{M}^T & & 0 & -\mu \\ & & & -\mu & 0 \end{pmatrix}, \quad (34)$$

where \mathcal{M} is an arbitrary 2×2 matrix that may be parametrized as

$$\mathcal{M} = \begin{pmatrix} -M_Z^x \cos \beta^x \sin \theta_W^x & M_Z^x \sin \beta^x \sin \theta_W^x \\ M_Z^x \cos \beta^x \cos \theta_W^x & -C^x M_Z^x \sin \beta^x \cos \theta_W^x \end{pmatrix}. \quad (35)$$

There are then seven parameters that enter neutralino events, and one must try to check the SUSY relations $M_Z^x = M_Z$, $\theta_W^x = \theta_W$ and $C^x = 1$. A general analysis is likely to be complicated. One possible simplification would be to consider a less than fully general neutralino mass matrix by setting, for example, $C^x = 1$. On the other hand, one might wish to assume the standard SUSY neutralino mass matrix, generalize the neutralino-fermion-sfermion coupling to g^{x^0} , and check that $g^{x^0} = g$. However, even this analysis is more complicated than the chargino case, because the SUSY neutralino mass matrix contains an additional parameter. In addition, an important caveat to all analyses based on the neutralino mass matrix is that such analyses rely on the absence of gauge singlets, and are therefore more model-dependent than the chargino analyses of previous sections.

Without detailed study, it is not possible to dismiss the possibility that precision studies of sfermion and neutralino properties may be useful for testing SUSY. However, even from the brief comments presented above, it is clear that the sfermion and neutralino sectors are significantly less promising than the chargino sector. Category (III) tests from chargino properties are likely to be the least model dependent and may be the first strong quantitative tests even if some other sparticles are lighter than charginos.

VII. CONCLUSIONS

Softly broken supersymmetric theories are like spontaneously broken gauge theories in that the relationships between dimensionless couplings implied by the symmetry continue to be preserved, while the corresponding relationships between the masses of various particles can be badly violated. It is this feature which provides the best opportunity for quantitative tests of supersymmetry. In this study we have examined the possibilities for testing various SUSY relations in a number of scenarios. These studies have been conducted in the experimental setting provided by a linear e^+e^- collider with polarizable beams, and results have been presented for $\sqrt{s} = 500 \text{ GeV}$ and integrated luminosities of 30 and 100 fb^{-1} .

In the scenario in which charginos are the first sparticles to be discovered, we have analyzed two representative cases. In the first, we probed the form of the chargino mass matrix, and in the second, we tested the $\tilde{\chi}_1^\pm f \tilde{f}$ coupling. In both examples, we found that the test led to rather strong quantitative confirmations of the MSSM and SUSY. As a by-product, interesting bounds on some SUSY parameters were also obtained. The availability of polarizable beams was found to play a vital role, allowing us to define characteristic regions, effectively eliminate dependences on certain SUSY parameters, and remove background. Our analysis was performed using a parton level Monte Carlo event generator and did not incorporate possible contamination of chargino pair events from other SUSY processes. Of course, a more detailed analysis that includes the simultaneous production of all possible SUSY events together with a more realistic simulation is needed before definitive conclusions about precision SUSY tests may be drawn.

The prospects for obtaining the first quantitative tests of SUSY from sfermion and neutralino properties were also considered. Sleptons were found to be poor candidates for such tests because of the difficulty in detecting sneutrinos, and precision tests from squarks were

found to rely on the discovery of at least four squarks or two squarks and, most likely, two Higgs bosons. The analysis of neutralino properties is complicated by its dependence on a large number of parameters. Whether these complications may be overcome in certain scenarios remains to be seen in further studies. However, while falsification of sfermion mass relations is the least model-dependent disproof of SUSY, it is likely that the chargino sector is the simplest and most powerful for verifying the quantitative predictions of SUSY.

We have not considered the possibilities for quantitative SUSY tests at other colliders, nor have we examined the additional constraints that come with the adoption of GUT and supergravity assumptions. Even with fairly weak assumptions, however, we have found that, if sparticles are produced at future e^+e^- colliders, measurements of their properties may allow us to quantitatively verify SUSY, a valuable first step in the exploration of the full structure of supersymmetric theories.

ACKNOWLEDGMENTS

The authors thank M. Drees, H. Haber, T. Rizzo, M. Strassler, and L. Susskind for enlightening conversations. H.M. was supported by the Director, Office of Energy Research, Office of High Energy and Nuclear Physics, Division of High Energy Physics of the U.S. Department of Energy under contract DE-AC03-76SF00098.

APPENDIX: UNCERTAINTY ANALYSIS

In this study we use the truncated forward-backward asymmetry $A^x \equiv A_i^x$, where $i = L$ or R , and the Y mode partial cross section σ_Y to constrain parameter space. These theoretical quantities are found through their correlations to experimental observables. The uncertainties in determining A^x and σ_Y therefore receive contributions from two sources: systematic errors, that is, uncertainties arising from the lack of perfect correlation between the theoretical quantities and the experimental observables, and experimental statistical errors. In this appendix we collect the formulae used to estimate the systematic and statistical errors.

Systematic errors are determined by performing Monte Carlo simulations at a number of points in parameter space. The truncated forward-backward asymmetry of chargino production before cuts, A^x , is determined through its correlation to A^{had} , the forward-backward asymmetry of the hadronic system's direction after cuts. The theoretical quantity A^x depends only on parameters that enter the production process, while A^{had} depends on both production and decay, and on cuts and detector effects. The systematic uncertainty in A^x is therefore determined by the sensitivity of A^{had} to the decay process, cuts, and detector effects, and this sensitivity is measured through simulations. For each of N_{pts} points in parameter space, A^x is determined from exact analytical expressions, and A^{had} is found from a Monte Carlo simulation. A linear fit to the resulting distribution in the (A^x, A^{had}) plane is parametrized by

$$A^{had} = aA^x + b \pm \Delta A_{MC}^{tot}, \quad (\text{A1})$$

where ΔA_{MC}^{tot} is the 1σ uncertainty in A^{had} for a fixed A^x . The total Monte Carlo uncertainty ΔA_{MC}^{tot} includes both the systematic error and fluctuations from finite Monte Carlo statistics. The contribution from Monte Carlo statistical fluctuations is

$$\Delta A_{MC}^{stat} = \left[\frac{1}{N_{pts}} \sum_{i=1}^{N_{pts}} (\Delta A_i^{had})^2 \right]^{\frac{1}{2}}, \quad (\text{A2})$$

where

$$\Delta A_i^{had} = \sqrt{\frac{1 - (A_i^{had})^2}{N_{MCi}}} \quad (\text{A3})$$

is the Monte Carlo statistical uncertainty in A_i^{had} for simulation i , and N_{MCi} is the effective number of events in simulation i . The systematic error of the distribution is then

$$\Delta A_{exp}^{sys} = \sqrt{(\Delta A_{MC}^{tot})^2 - (\Delta A_{MC}^{stat})^2}. \quad (\text{A4})$$

To the systematic error must be added the experimental statistical error. This error is given by

$$\Delta A_{exp}^{stat} = \sqrt{\frac{1 - (A^{had})^2}{N_{exp}} + \frac{(1 - A^{had})^2 N_{back}}{N_{exp}^2}}, \quad (\text{A5})$$

where A^{had} is the forward-backward asymmetry for our case study, and N_{exp} (N_{back}) is the number of signal (background) events that pass all cuts and is proportional to the integrated luminosity. (Here we have assumed that the background is well-understood and may be subtracted up to statistical uncertainties. We also assume that all background events are in the forward hemisphere, a good approximation for the dominant background, W pair production.) We estimate the total experimental uncertainty in A^{had} for a given A^x to be

$$\Delta A_{exp}^{tot} = \sqrt{(\Delta A_{exp}^{sys})^2 + (\Delta A_{exp}^{stat})^2}. \quad (\text{A6})$$

What we actually measure is A^{had} , however. We therefore are more interested in the experimental uncertainty in A^x for a fixed A^{had} , which is

$$\Delta A^x = |a|^{-1} \Delta A_{exp}^{tot}, \quad (\text{A7})$$

where a is the slope of the linear fit in Eq. (A1).

The efficiency of the cuts η is found simply by its correlation to previous measurements. To determine the uncertainty in η , we reduce the parameter space to the region in which the previous measurements have their appropriate values and determine the variation of η within this subspace. We determine η for each of the simulations and obtain a distribution of points in the (A^x, η) plane. The best linear fit to this distribution is

$$\eta = a' A^x + b' \pm \Delta \eta_{MC}^{tot}, \quad (\text{A8})$$

where $\Delta\eta_{MC}^{tot}$ is the 1σ error in η for a fixed A^x . To find the systematic error, we must again remove the fluctuations that arise solely from finite Monte Carlo statistics. The Monte Carlo statistical error is

$$\Delta\eta_{MC}^{stat} = \left[\frac{1}{N_{pts}} \sum_{i=1}^{N_{pts}} (\Delta\eta_i)^2 \right]^{\frac{1}{2}}, \quad (\text{A9})$$

where the statistical error for simulation i is given by

$$\Delta\eta_i = \sqrt{\frac{\eta_i(1-\eta_i)}{N_{MC}}}. \quad (\text{A10})$$

The systematic error in η for a fixed A^x is then

$$\Delta\eta^{sys} = \sqrt{(\Delta\eta_{MC}^{tot})^2 - (\Delta\eta_{MC}^{stat})^2}. \quad (\text{A11})$$

However, as seen above, A^x is not determined exactly. The uncertainty in A^x weakens the determination of η , and the total uncertainty in η is

$$\Delta\eta = \sqrt{(a'\Delta A^x)^2 + (\Delta\eta^{sys})^2}. \quad (\text{A12})$$

We must now convert the uncertainty in η into an uncertainty in σ_Y . The Y mode partial cross section and its fractional uncertainty are given by

$$\sigma_Y = N_{exp}\eta^{-1}\mathcal{L}^{-1} \quad (\text{A13})$$

and

$$\frac{\Delta\sigma_Y}{\sigma_Y} = \left[\left(\frac{\Delta N_{exp}}{N_{exp}} \right)^2 + \left(\frac{\Delta\eta}{\eta} \right)^2 + \left(\frac{\Delta\mathcal{L}}{\mathcal{L}} \right)^2 \right]^{\frac{1}{2}}, \quad (\text{A14})$$

where \mathcal{L} is the integrated luminosity. For the purposes of this study, $\Delta\mathcal{L}/\mathcal{L}$ is negligible. The uncertainty in the number of Y events passing the cuts is $\Delta N_{exp} = \sqrt{N_{exp} + N_{back}}$, where N_{exp} (N_{back}) is the number of Y mode (background) events passing the cuts, respectively, and we have again assumed that the background is well-understood and may be subtracted up to statistical uncertainties.

REFERENCES

- [1] A.E. Faraggi, J.S. Hagelin, S. Kelley, and D.V. Nanopoulos, *Phys. Rev. D* **45**, 3272 (1992).
- [2] S. Martin and P. Ramond, *Phys. Rev. D* **48**, 5365 (1993).
- [3] Y. Kawamura, H. Murayama, and M. Yamaguchi, *Phys. Lett.* **324B**, 52 (1994).
- [4] G. Loew, in *Proceedings of the ECFA Workshop on e^+e^- Linear Colliders (LC92)*, Garmisch Partenkirchen, Germany, July 25 – August 2, 1992, edited by R. Settles, MPI-PHE/93-14, ECFA 93-154 (1993), Vol. 2, p. 481.
- [5] *Proceedings of the Workshop on Physics and Experiments with Linear Colliders*, Saariselka, Finland, 1991, edited by R. Orava, P. Eerola, and M. Nordberg (World Scientific, River Edge, New Jersey, 1992).
- [6] JLC Group, *JLC-I*, Tsukuba, Japan, 1992 (KEK Report 92-16, Tsukuba, 1992).
- [7] *Workshop on e^+e^- Collisions at 500 GeV: The Physics Potential*, edited by P. M. Zerwas, DESY 92-123A,B,C (1992/1993).
- [8] *Proceedings of the Workshop on Physics and Experiments with Linear e^+e^- Colliders*, Waikoloa, Hawaii, 1993, edited by F.A. Harris, S.L. Olsen, S. Pakvasa, and X. Tata (World Scientific, Singapore, 1993).
- [9] A. Leike, *Int. J. Mod. Phys. A* **4**, 845 (1989).
- [10] T. Tsukamoto, K. Fujii, H. Murayama, M. Yamaguchi, and Y. Okada, KEK Report No. 93-146, 1993, to appear in *Phys. Rev. D*.
- [11] S. Orito, in Ref. [8], Vol. I, p. 230.
- [12] R. Becker and C. Vander Velde, in Ref. [8], Vol. II, p. 808.
- [13] T. Kon, in Ref. [8], Vol. II, p. 822.
- [14] J.L. Feng and D.E. Finnell, *Phys. Rev. D* **49**, 2369 (1994).
- [15] M.E. Peskin, to appear in *Proceedings of the 22nd INS International Symposium on Physics with High Energy Colliders*, Tokyo, Japan, March 8-10, 1994, SLAC-PUB-6582 (1994).
- [16] J.L. Feng and M.J. Strassler, SLAC-PUB-6497, RU-94-67 (1994), to appear in *Phys. Rev. D*.
- [17] For reviews of supersymmetry and the minimal supersymmetric standard model, see H.E. Haber and G.L. Kane, *Phys. Rep.* **117**, 75 (1985); H.P. Nilles, *Phys. Rep.* **110**, 1 (1984); P. Nath, R. Arnowitt, and A.H. Chamseddine, *Applied N = 1 Supergravity*, ICTP Series in Theoretical Physics, Vol. 1 (World Scientific, Singapore, 1984); X. Tata, in *The Standard Model and Beyond*, proceedings of the Ninth Symposium on Theoretical Physics, Mt. Sorak, Korea, 1990, edited by J.E. Kim (World Scientific, River Edge, New Jersey, 1991), p. 304.
- [18] S. Dimopoulos and H. Georgi, *Nucl. Phys.* **B193**, 150 (1981).
- [19] L. Girardello and M.T. Grisaru, *Nucl. Phys.* **B194**, 65 (1982).
- [20] J. Ellis and D.V. Nanopoulos, *Phys. Lett.* **110B**, 44 (1982); T. Inami and C.S. Lim, *Nucl. Phys.* **B207**, 533 (1982); M.J. Duncan and J. Trampetic, *Phys. Lett.* **134B**, 439 (1984); J. Hagelin, S. Kelley, and T. Tanaka, *Nucl. Phys.* **B415**, 293 (1994).
- [21] J.F. Gunion and H.E. Haber, *Phys. Rev. D* **37**, 2515 (1988).
- [22] Particle Data Group, L. Montanet *et al.*, *Phys. Rev. D* **50**, 1173 (1994).
- [23] OPAL Collaboration, M. Akrawy *et al.*, *Phys. Lett.* **240B**, 261 (1990); DELPHI Collaboration, P. Abreu *et al.*, *Phys. Lett.* **247B**, 157 (1990); ALEPH Collaboration, D.

- Décamp *et al.*, Phys. Rep. **216**, 253 (1992); L3 Collaboration, O. Adriani *et al.*, Phys. Rep. **236**, 1 (1993).
- [24] See, for example, P. Janot, in Ref. [8], Vol. I, p. 192, and H. Haber, to appear in *Proceedings of Beyond the Standard Model IV*, Lake Tahoe, California, December 13-18, 1994.
- [25] J.-F. Grivaz, in Ref. [5], Vol. I, p. 353.
- [26] M. Nojiri, KEK Report No. KEK-TH-425 (1994).

FIGURES

FIG. 1. The diagrams contributing to chargino production at e^+e^- colliders. The $\tilde{\nu}_e$ t -channel diagram is absent for e_R^- beams.

FIG. 2. Contours of constant σ_R (in fb) for fixed $\tan\beta = 4$ in the (μ, M_2) plane. Chargino production is inaccessible for $\sqrt{s} = 500$ GeV in the hatched region, and the cross-hatched region is excluded by the current experimental mass limit $m_{\tilde{\chi}_1^\pm} > 45$ GeV. The cross section σ_R quickly drops to zero in the $|\mu| \lesssim M_2$ regions.

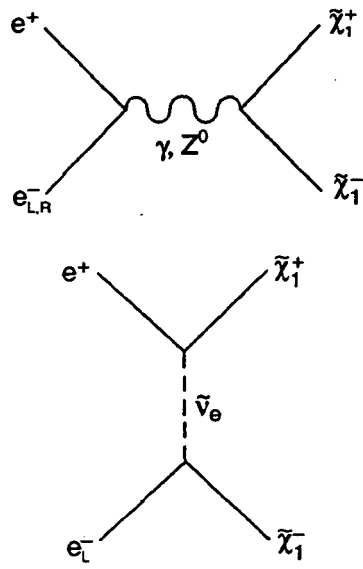
FIG. 3. The three characteristic regions for fixed $\tan\beta = 4$ in the (μ, M_2) plane, as defined in the text. (The corresponding $\mu > 0$ parts of these regions are unlabeled.) The hatched and cross-hatched regions are as in Fig. 2. The dashed curve is the contour $m_{\tilde{\chi}_1^\pm} = 172$ GeV.

FIG. 4. The correlation of A^{had} and A_R^X for 38 points in the seven-dimensional parameter space $(\mu, M_2, \tan\beta^x, M_1, m_{\tilde{t}}, m_{\tilde{q}}, M_{\tilde{W}}^X)$. These points have been picked randomly, subject only to the constraints that $m_{\tilde{\chi}_1^\pm}$, $m_{\tilde{\chi}_1^0}$, and $m_{\tilde{\chi}_2^\pm}$ are within 2 GeV of their underlying values in the case study. The linear best fit is given by the solid line, and the 1σ deviations are given by the dashed lines.

FIG. 5. The correlation of η and A_R^X for the 38 points in the seven-dimensional parameter space $(\mu, M_2, \tan\beta^x, M_1, m_{\tilde{t}}, m_{\tilde{q}}, M_{\tilde{W}}^X)$, selected as in Fig. 4. The linear best fit is given by the solid line, and the 1σ deviations are given by the dashed lines.

FIG. 6. The allowed region of the (ϕ_+, ϕ_-) plane from measurements of A_R^X and σ_Y . The lightly (heavily) shaded region is allowed for $\mathcal{L}_R = 30$ (100) fb^{-1} . Contours of constant $M_{\tilde{W}}^X$ are plotted in GeV. On the dotted contours, the SUSY relation $M_{\tilde{W}}^X = M_W$ holds.

FIG. 7. Allowed regions (shaded) of the $(m_{\tilde{\nu}}, g^x)$ plane for $\mathcal{L}_L =$ (a) 30 fb^{-1} and (b) 100 fb^{-1} . Solid (dashed) curves are contours of constant σ_L (A_L^X) that bound the allowed regions. On the dotted lines, the SUSY relation $g^x = g$ is satisfied.



10-94

7790A04

Fig. 1

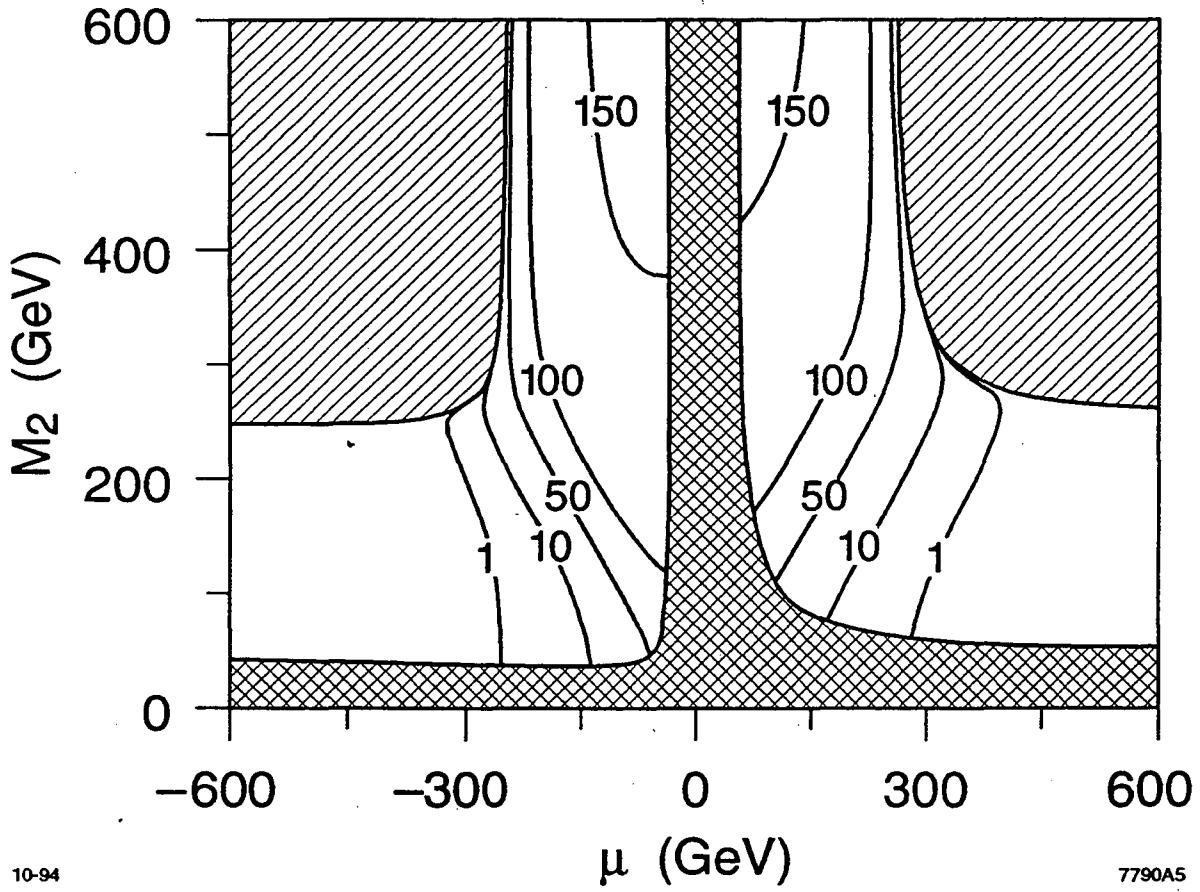


Fig. 2

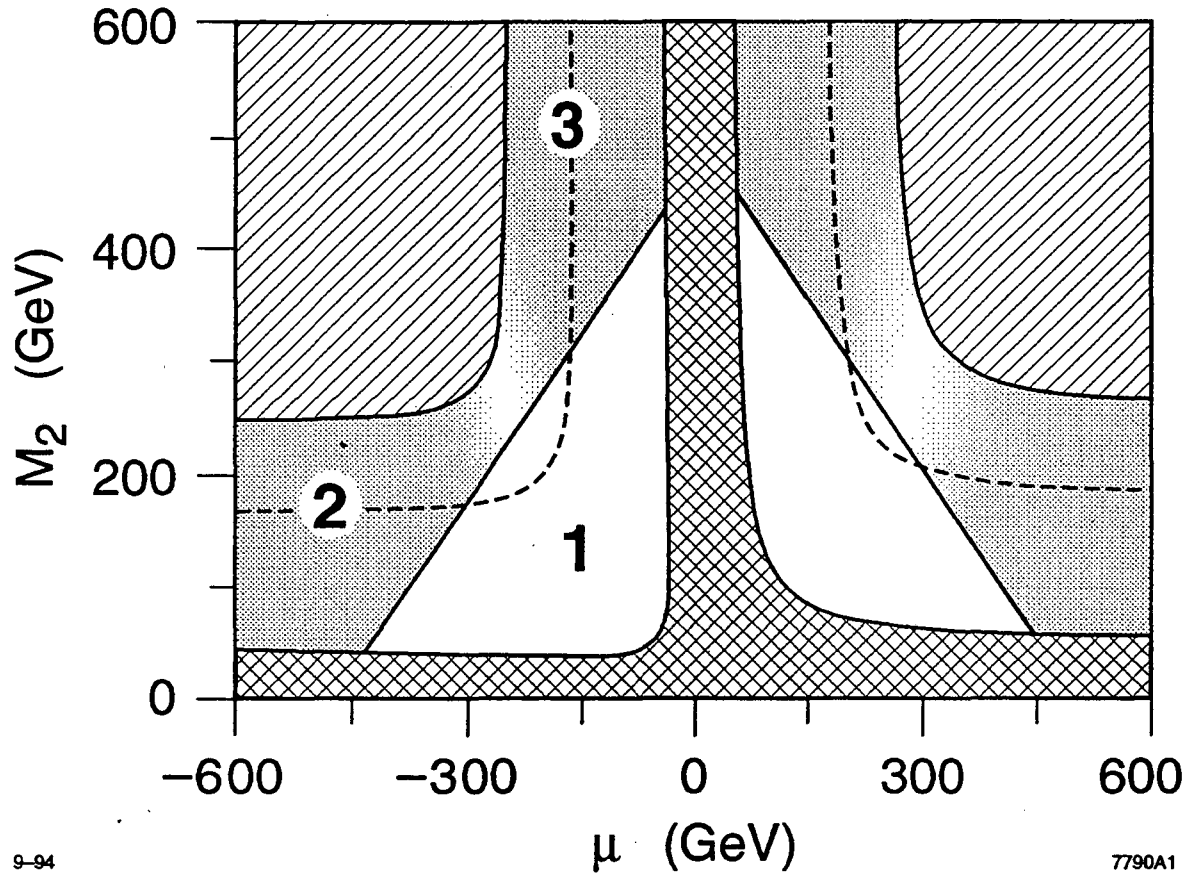
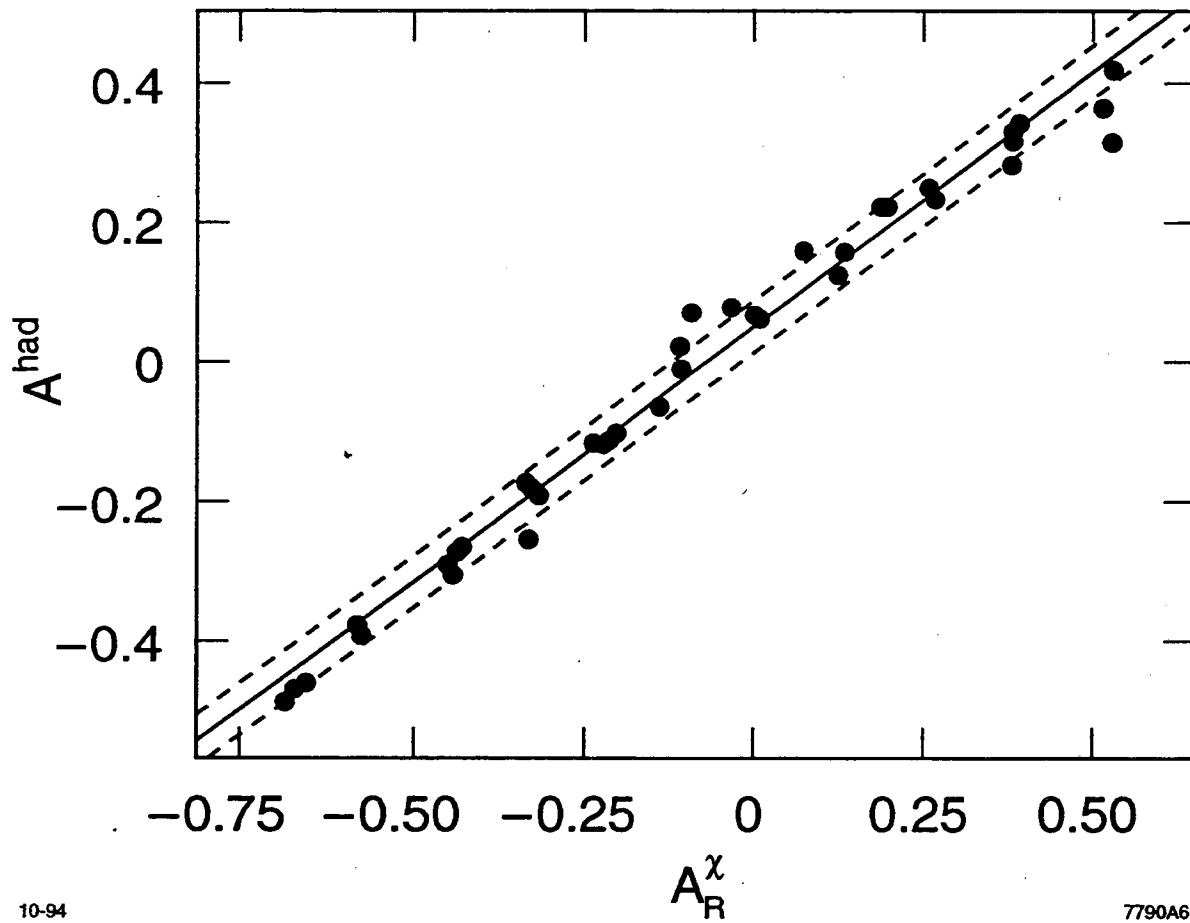


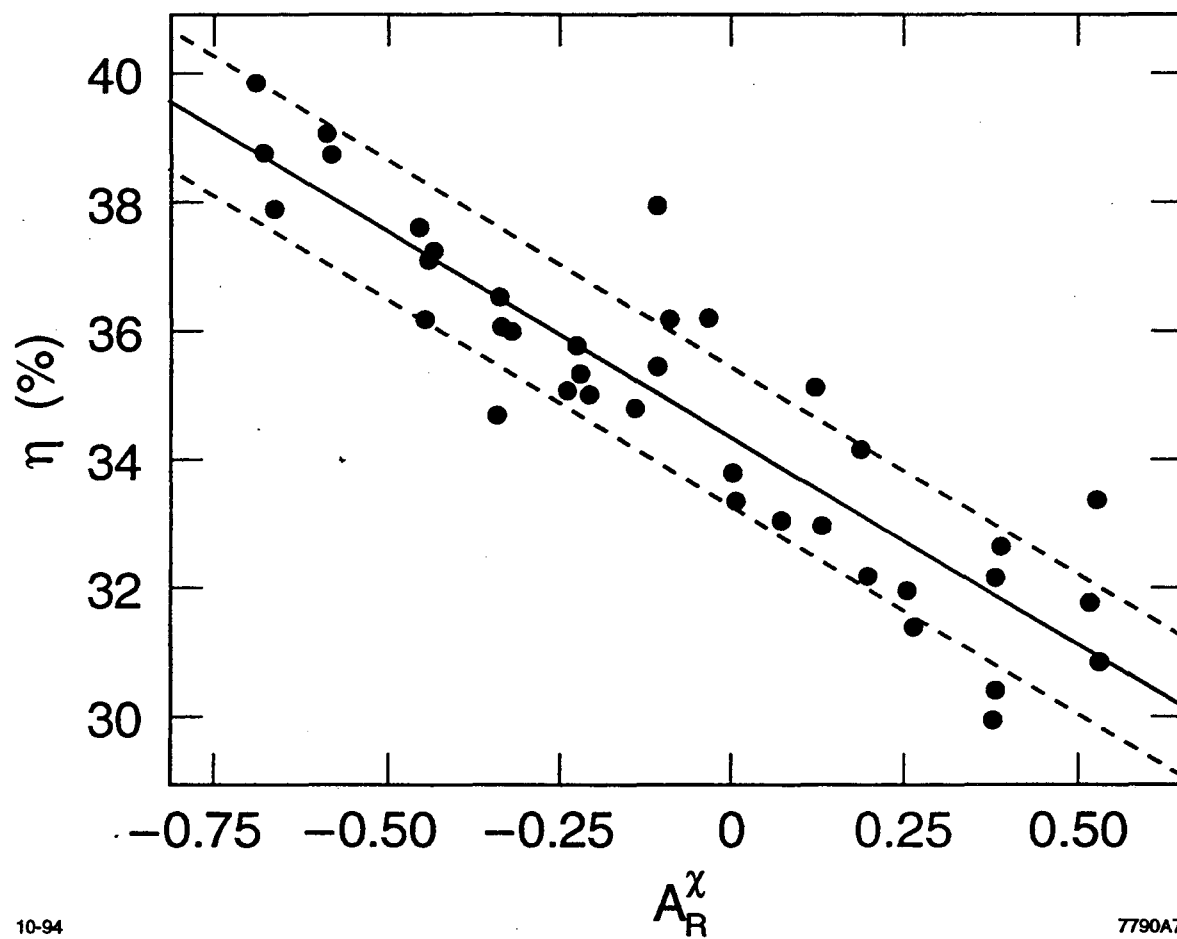
Fig. 3



10-94

7790A6

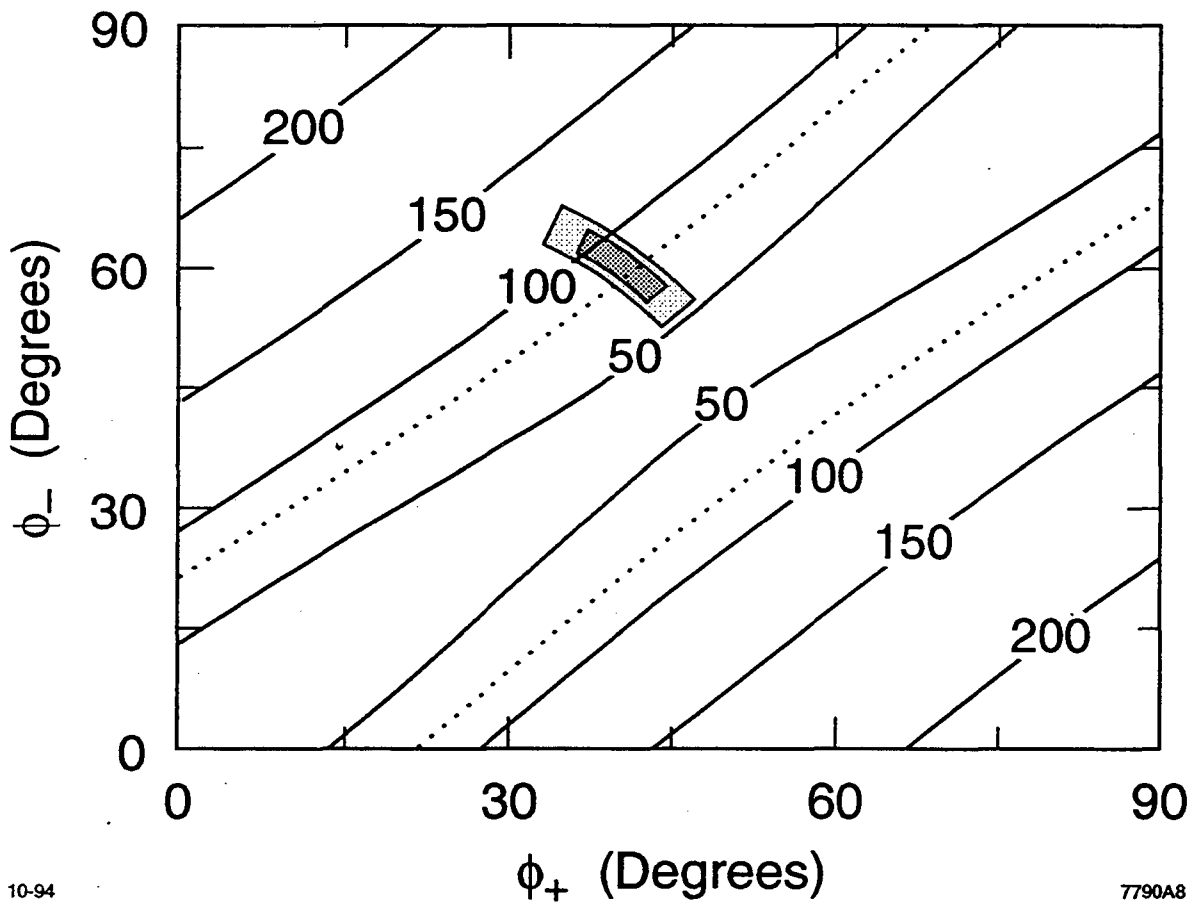
Fig. 4



10-94

7790A7

Fig. 5



10-94

7790A8

Fig. 6

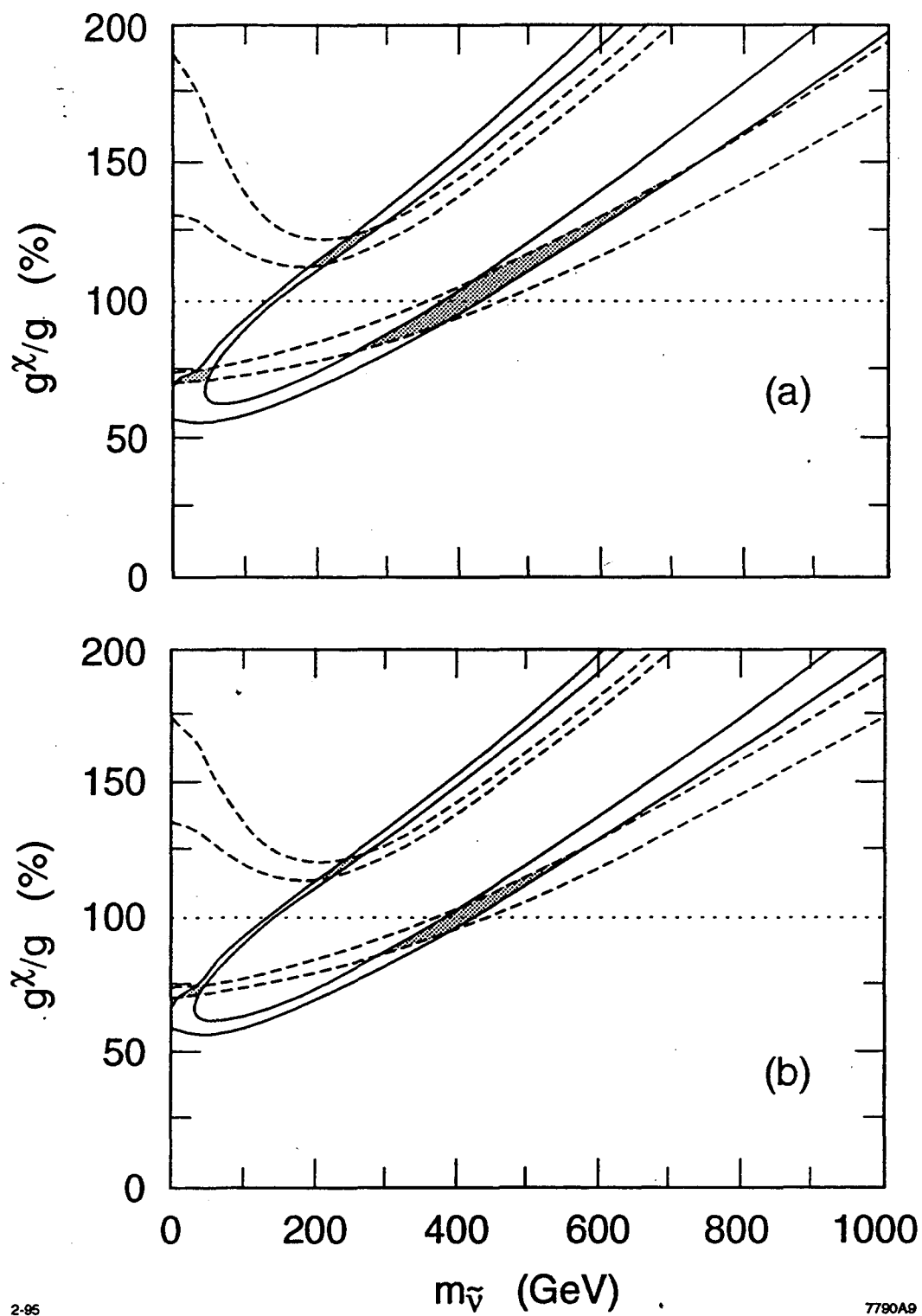


Fig. 7

LAWRENCE BERKELEY LABORATORY
UNIVERSITY OF CALIFORNIA
TECHNICAL INFORMATION DEPARTMENT
BERKELEY, CALIFORNIA 94720